連星系からの高エネルギー放射

山梨学院大学
内藤統也

宇宙線研究所共同利用研究会
「高エネルギー宇宙物理学の将来とCTA」
2010年1月9日 (土)

4 VHE Gamma-ray binaries

- PSR B1259−63/SS2883
- LS I +61 303
- LS 5039
- Cygnus X-1

Jet

Disc-PSR interraction

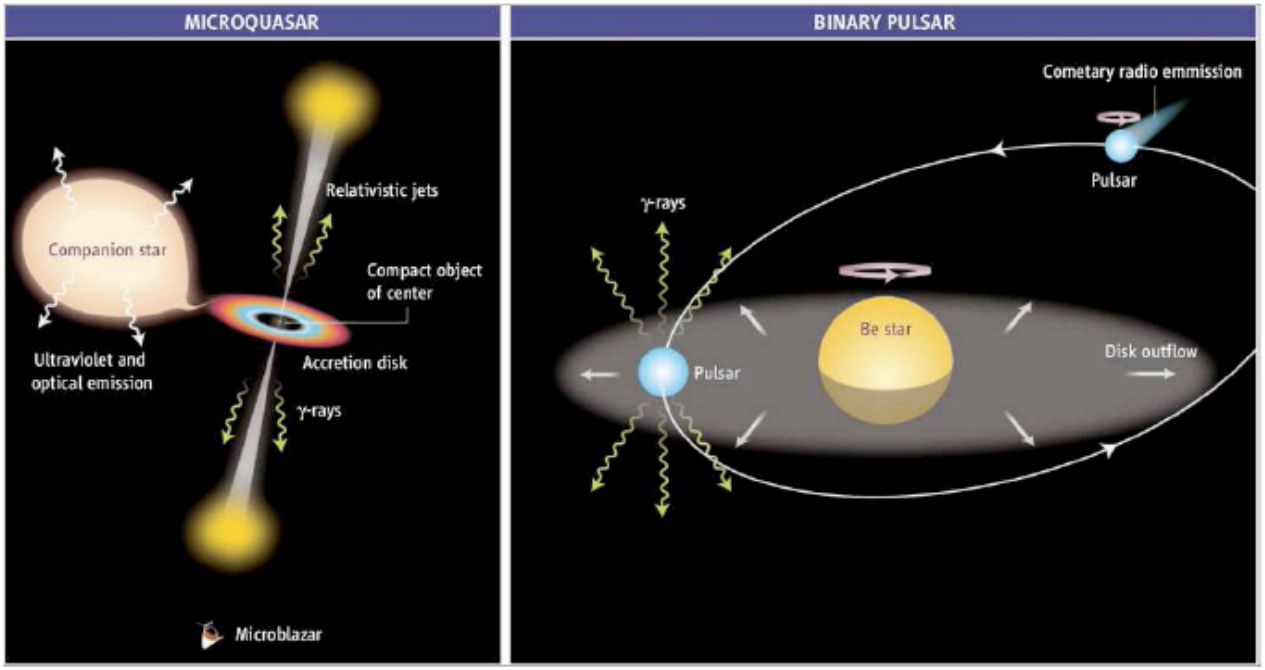

Fig. 3 Alternative models for very energetic gamma-ray binaries. *Left*: Microquasars are powered by compact objects (neutron stars or stellar-mass black holes) via mass accretion from a companion star. The jets boost the energy of stellar winds to the range of very energetic gamma-rays. *Right*: Pulsar winds are powered by rotation of neutron stars; the wind flows away to large distances in a comet-shape tail, as has been shown in [14] to be the case for LS I +61 303. Interaction of this wind with the companion-star outflow may produce very energetic gamma-rays.

I. F. Mirabel (2006)

目次

- ４つの連星系
  - PSR B1259−63/SS2883, LS I +61 303, LS 5039, Cygnus X-1
- 新しいTeVソース
  - HESS J0632+057
  - 共通点
- 未知のTeVソースの可能性
  - HMXBs
  - Massive star Binary

Nature of 4 binaries

	PSR B1259–63 /SS2883	LS I +61 303	LS 5039	Cygnus X-1
System Type	Be+NS	Be+NS/BH?	O+BH?	O+BH
Distance (kpc)	1.5	2.0	2.5	2.2
Orbital Period (d)	1237	26.5	3.9	5.6
Eccentricity	0.87	0.72	0.35	~0
Periastron-apastron (AU)	0.7–10	0.1–0.7	0.1–0.2	0.2
$M_{compact}$ (M_o)	1.4	1–4	1.4–5	20±5
L_{VHE} (10^{33} erg s^{-1})	2.3	8	7.8	12
Γ_{VHE}	2.7±0.2	2.6±0.2	2.06±0.05	3.2±0.6
Origin of Gamma-ray	disc-PSR interraction	disc-PSR and/or Jet	Jet?	flare (Jet?)

LS I +61 303

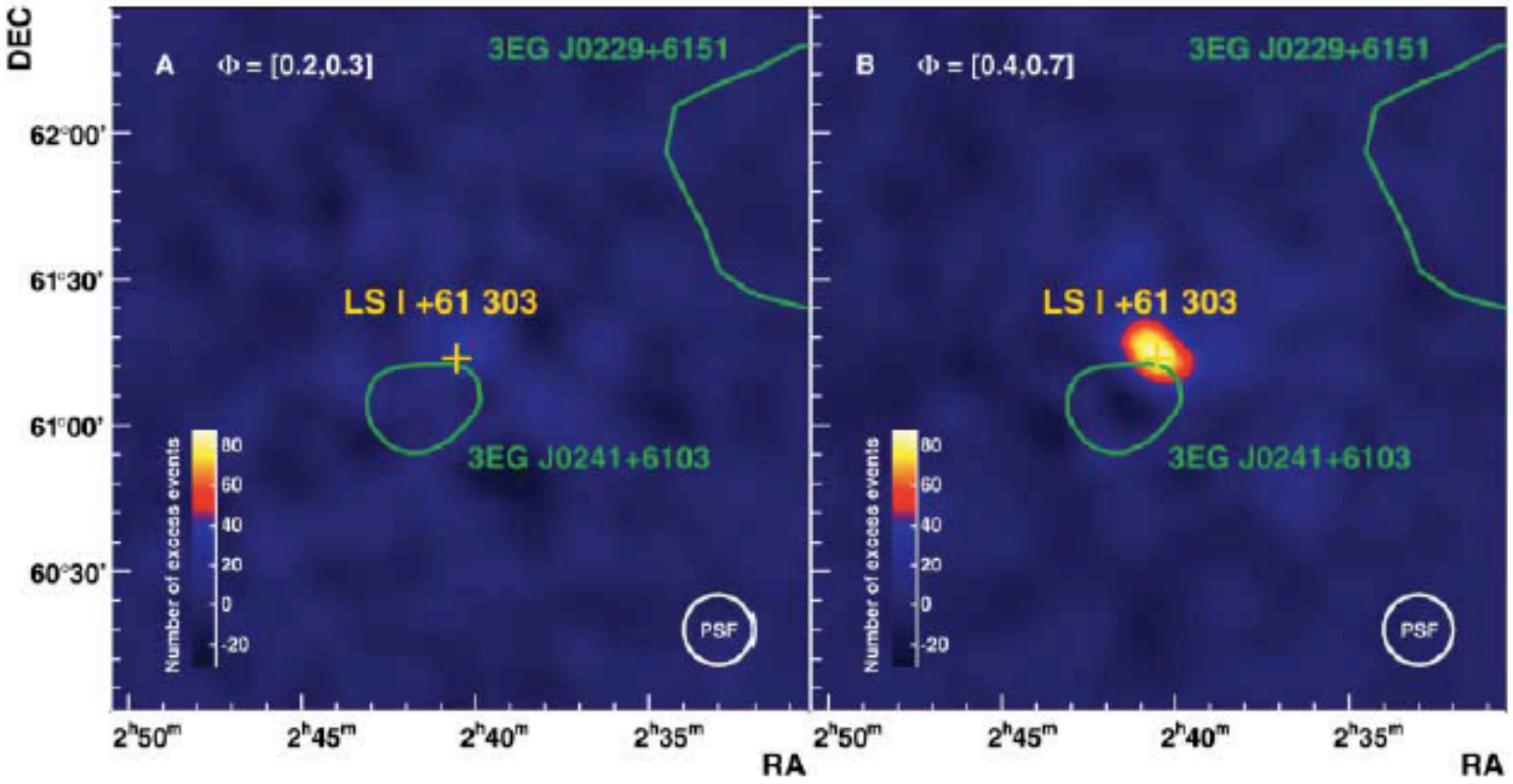

MAGIC: TeV
Albert 2006

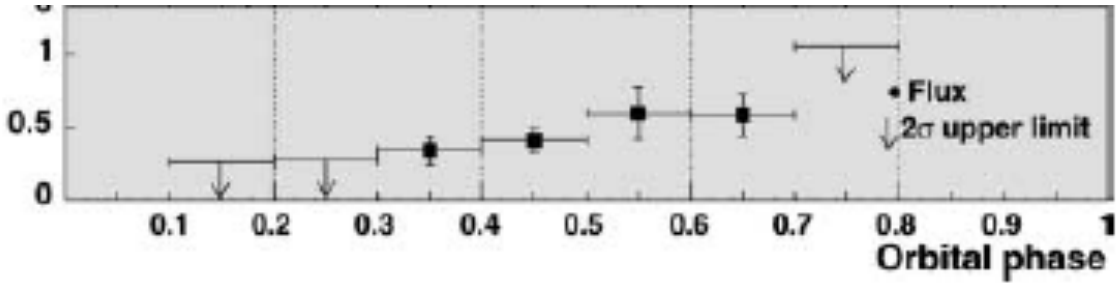

LS I +61 303: radio

- Dhawan et al. (Proceedings of the VI Microquasar Workshop)

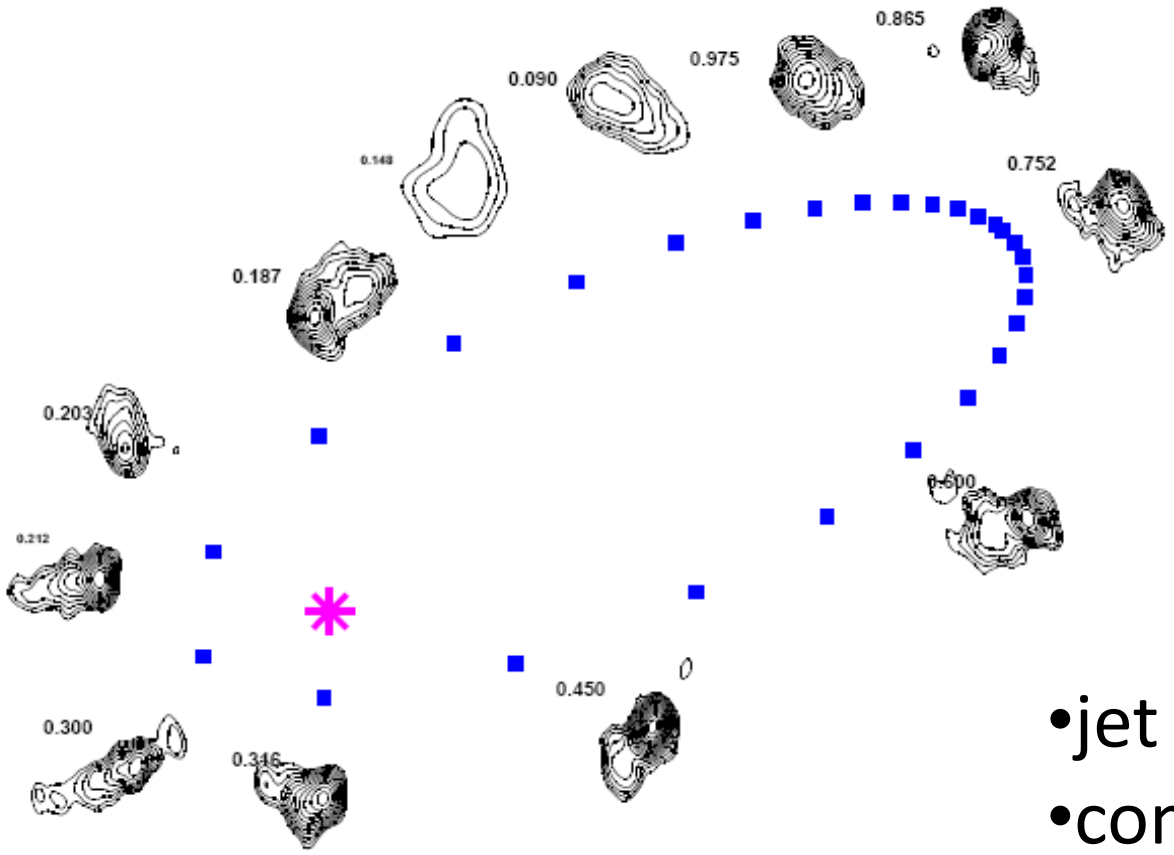

- jet like?
- cometary tail?

LS I +61 303: Flare

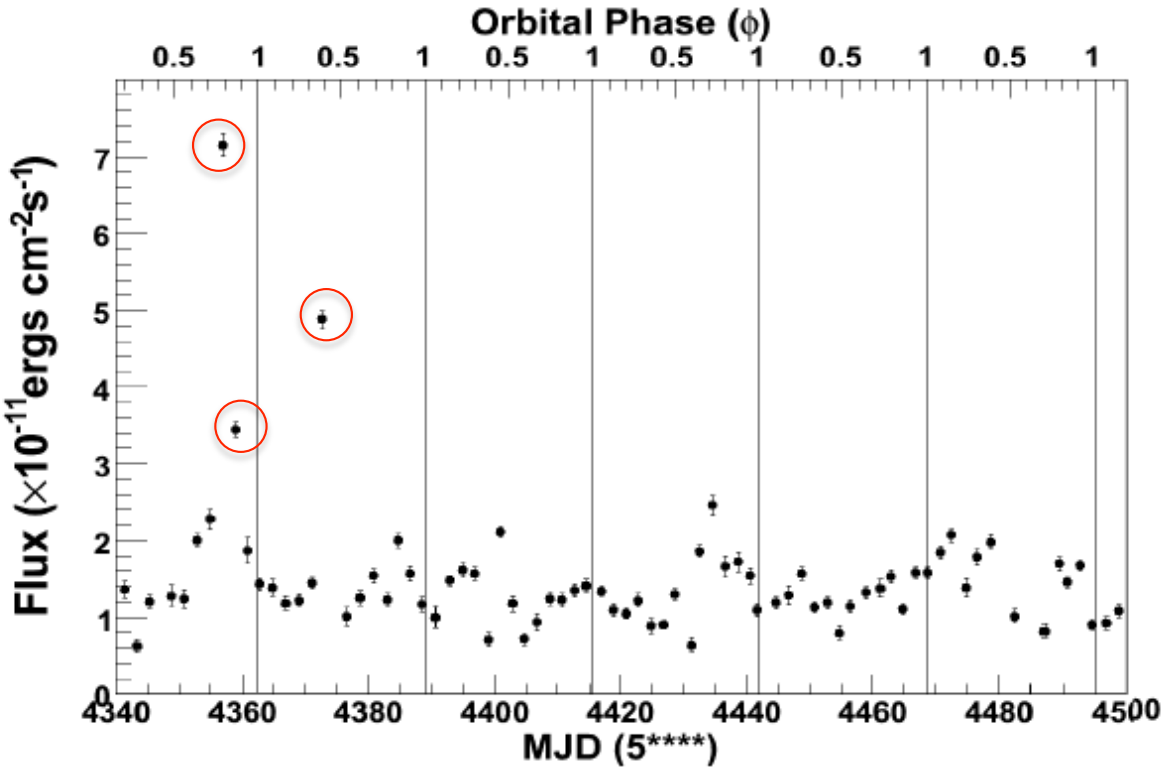

Smith et al. 2008

	Flare	MJD (UTC)	Usable Data (s)	PCUs	α	Flux (2-10 keV) (10^{-11}erg cm^{-2} s^{-1})
2007/09/13	Flare 1	54356 (11:09-11:25)	528	2,4	1.4±0.1	7.2±0.2
2007/09/15	Flare 2	54358 (10:13-10:28)	560	2,3,4	1.7±0.1	3.5±0.1
2007/09/29	Flare 3	54372 (03:31-03:35)	553	2,4	1.6±0.1	4.9±0.1

LS I +61 303: Burst

- Swift-BAT

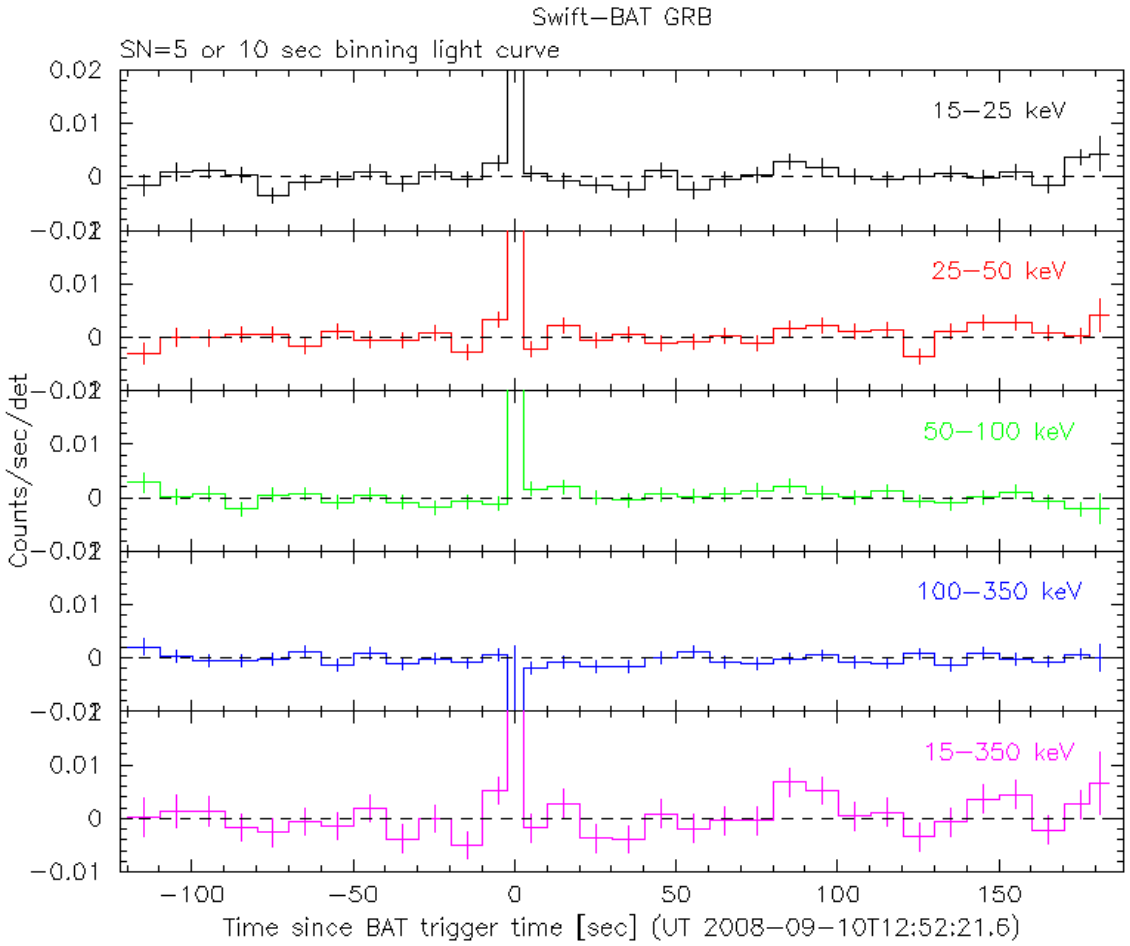

http://gcn.gsfc.nasa.gov/notices_s/324362/BA/

Burst detected by
Swift-BAT
2008.09.10
short burst: 0.23s

ATel #1715;
Dubus & Giebels 2008

SGR?

LS I +61 303: QPO?

- RXTE

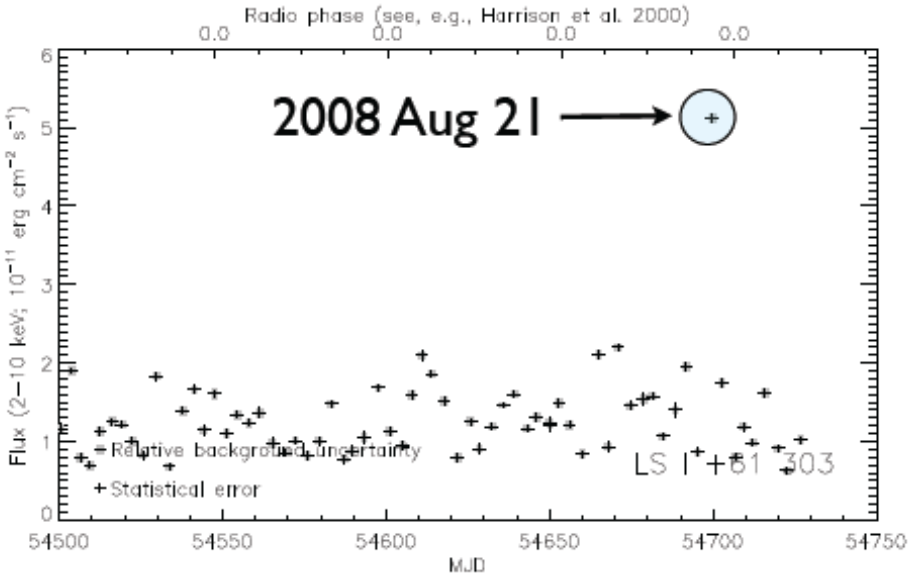

Time series (1 s bins) from 2008 Aug 21

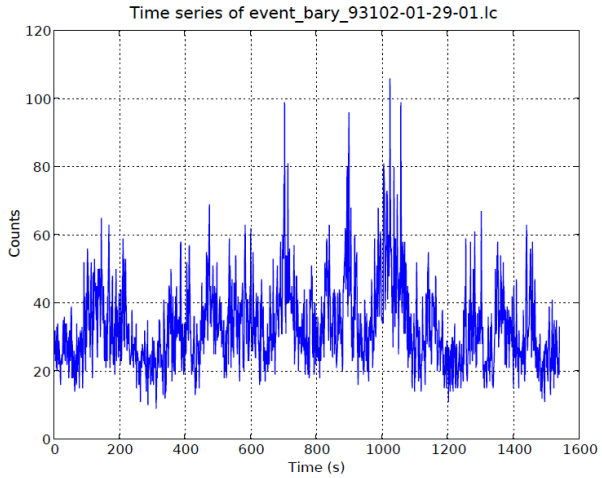

Flare detected by
RXTE-PCA
2008.08.21

ATel #1730, Ray et al

unusual X-ray activity

QPO?

http://heasarc.gsfc.nasa.gov/docs/xte/RXTEworkshop/Ray_RXTEworkshop09.pdf

Cygnus X-1からの TeV flare

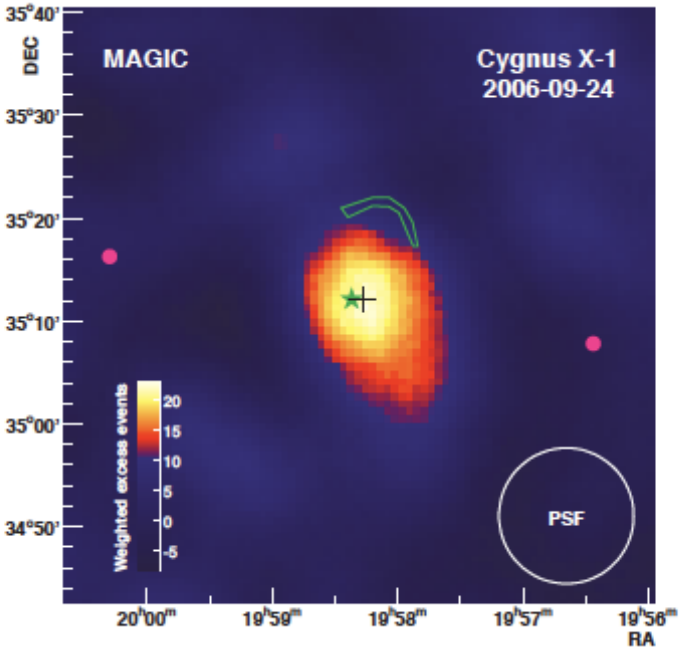

FIG. 3.— Gaussian-smoothed ($\sigma = 4'$) map of γ-ray excess events (background subtracted) above 150 GeV around Cygnus X-1 corresponding to 78.9 minutes EOT between MJD 54002.928 and 54002.987 (2006-09-24). The black cross shows the best-fit position of the γ-ray source. The position of the X-ray source and radio emitting ring-like are marked by the green star and contour, respectively. The purple dots mark the directions tracked during the observations. Note that the bin contents are correlated due to the smoothing.

flare
→LS I +61 303と同じ放射過程？

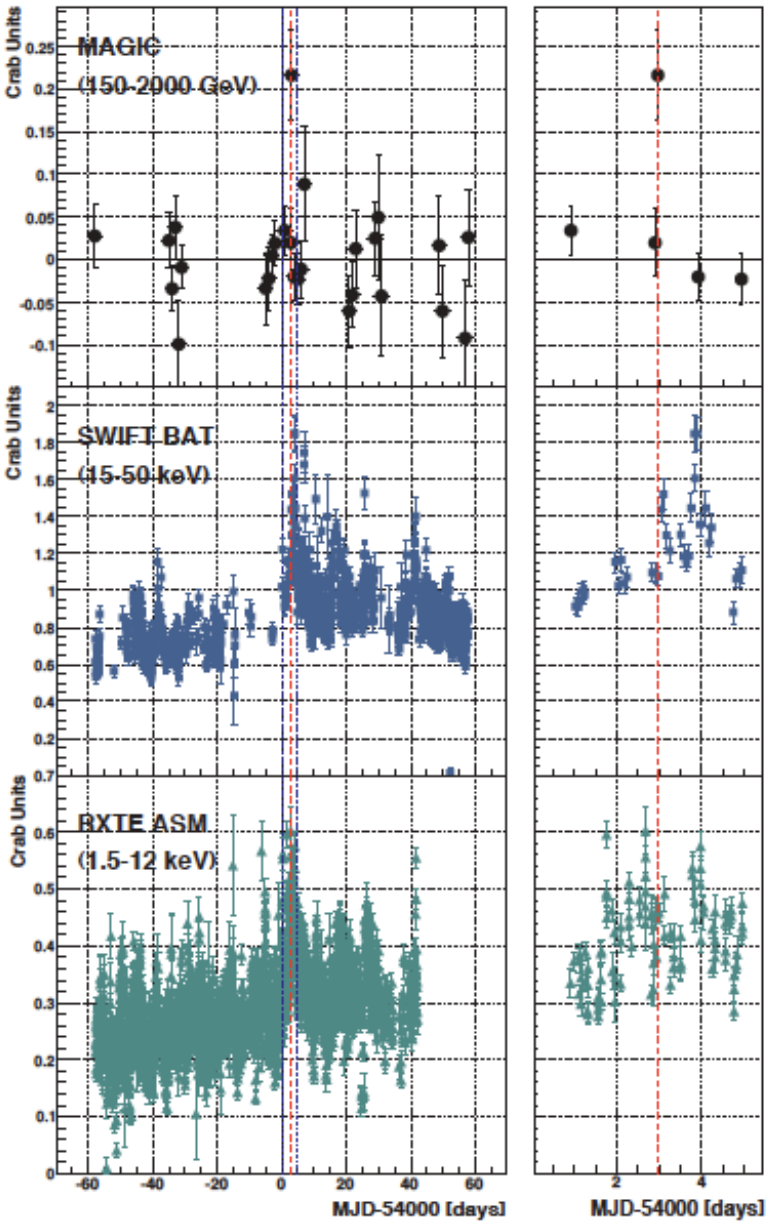

FIG. 4.— From top to bottom: MAGIC, *Swift*/BAT (from http://swift.gsfc.nasa.gov/docs/swift/results/transients/) and *RXTE*/ASM (from http://heasarc.gsfc.nasa.gov/xte_weather/) measured fluxes from Cygnus X-1 as a function of the time. The left panels show the whole time spanned by MAGIC observations. The vertical, dotted blue lines delimit the range zoomed in the right panels. The vertical red line marks the time of the MAGIC signal.

jet-clump model

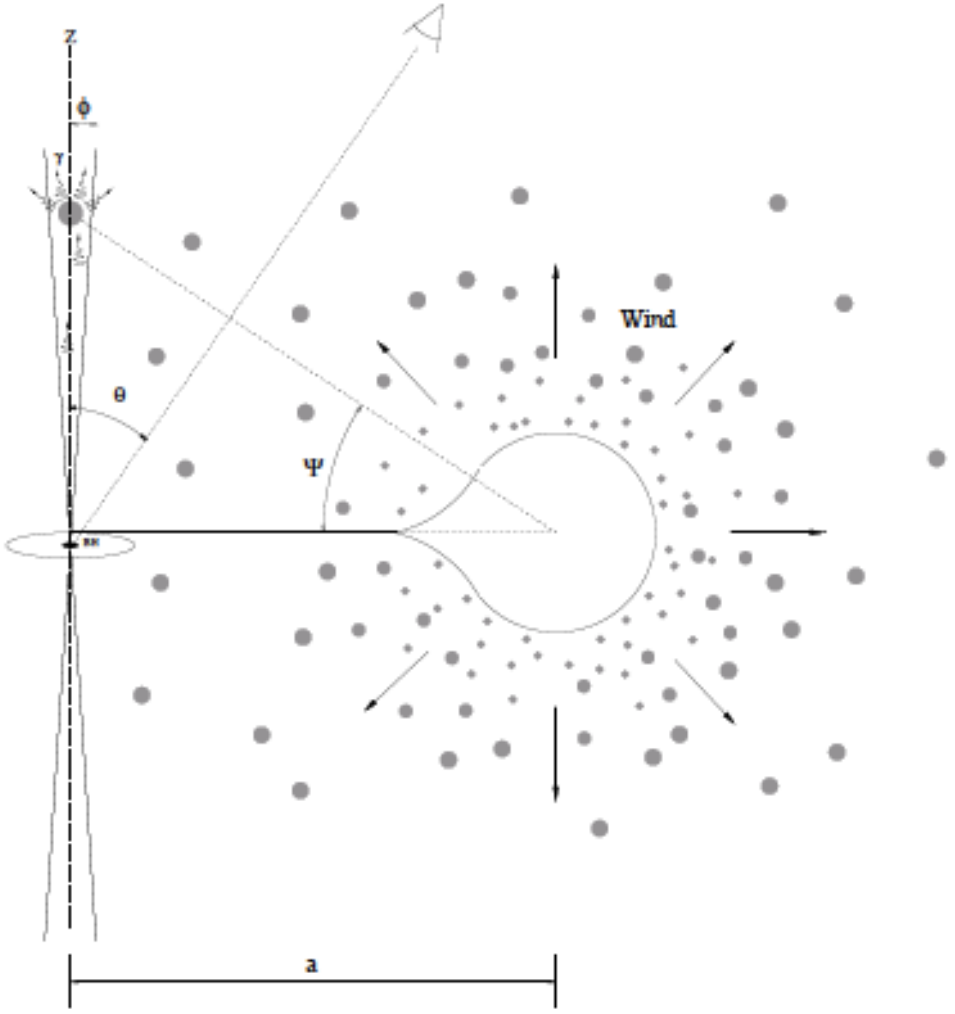

FIG. 1.— Sketch of the assumed model, described further in the text.

Owocki et al. 2009

$$\text{clump column } N_c = 3 \times 10^{21}\text{cm}^{-2}$$

$$\tau_c = \sigma N_c \approx 10^{-4}$$

$$L_\gamma = q_i \tau_c L_i \approx 10^{32}\,\text{erg}\,\text{s}^{-1}$$

LS 5039: TeV

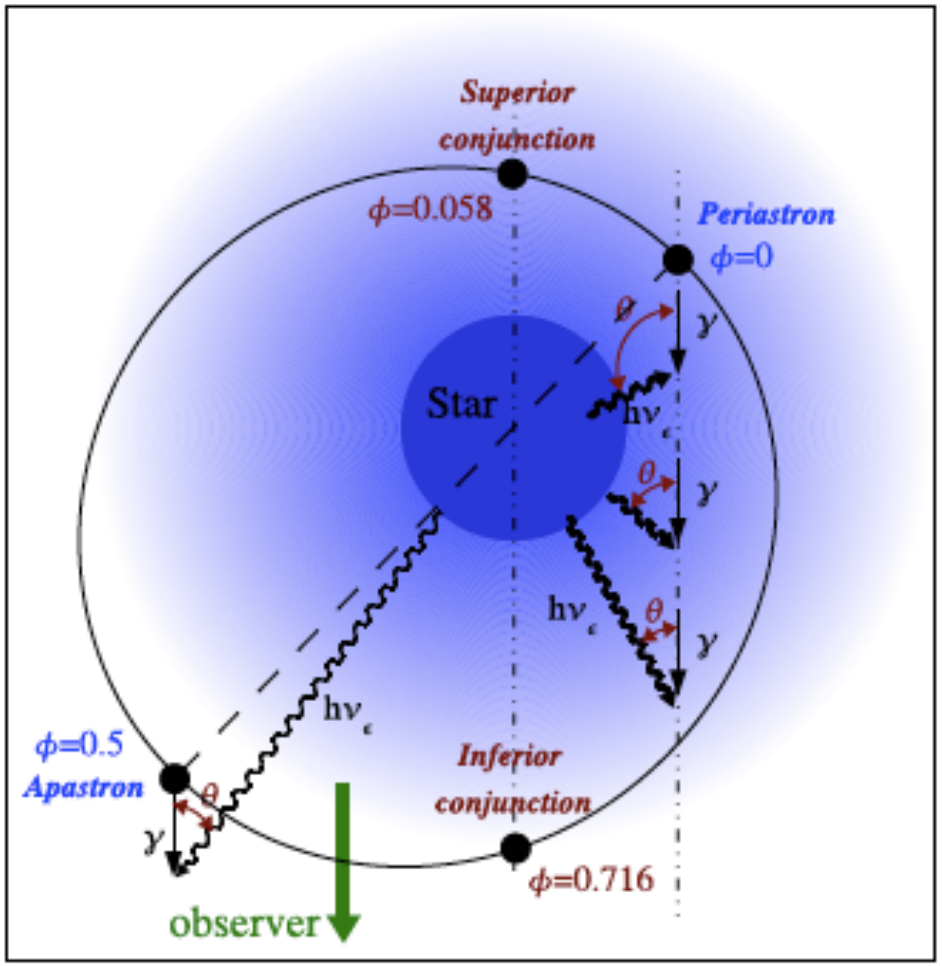

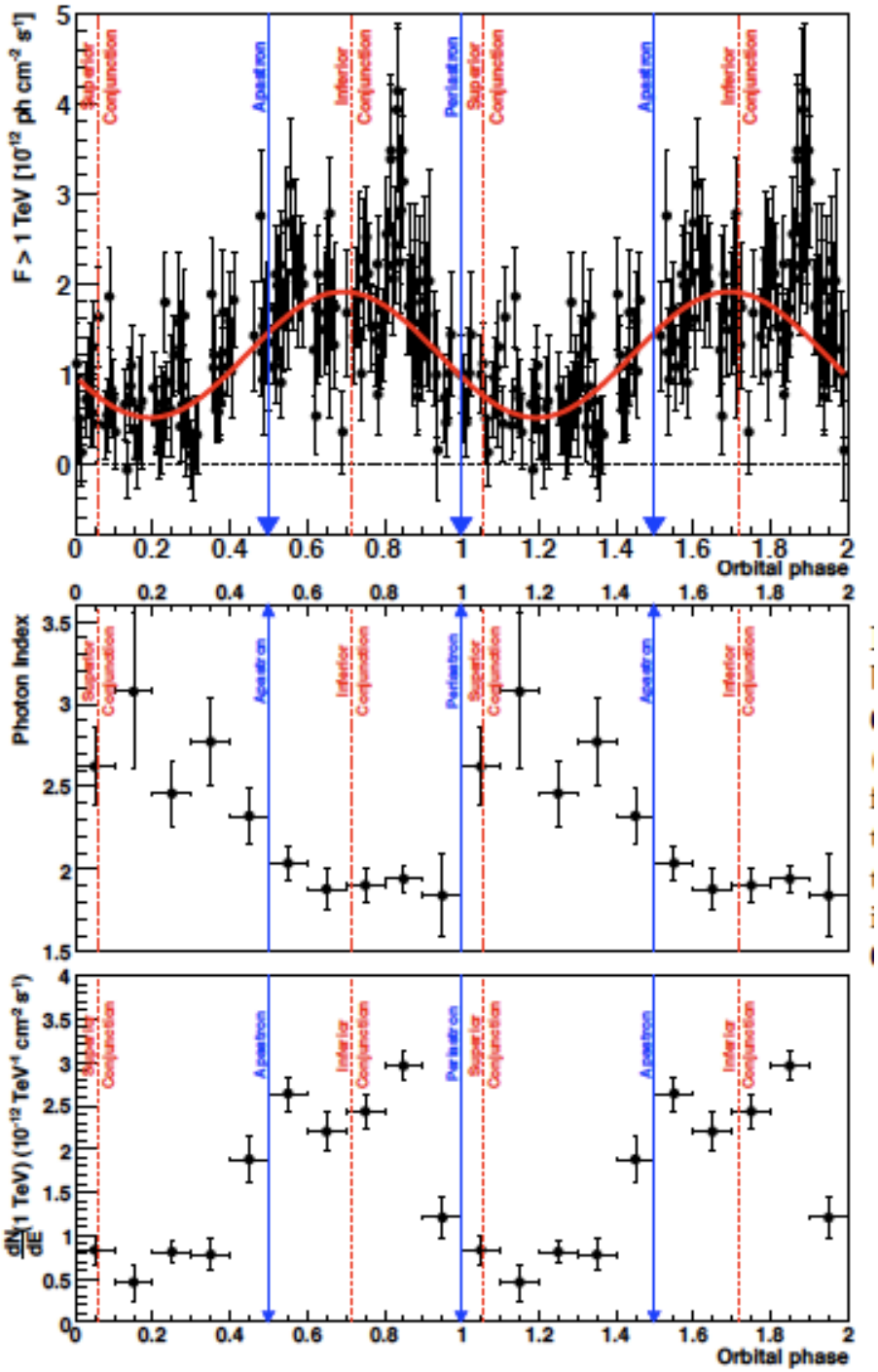

Aharonian et al. 2006

LS 5039のjet構造

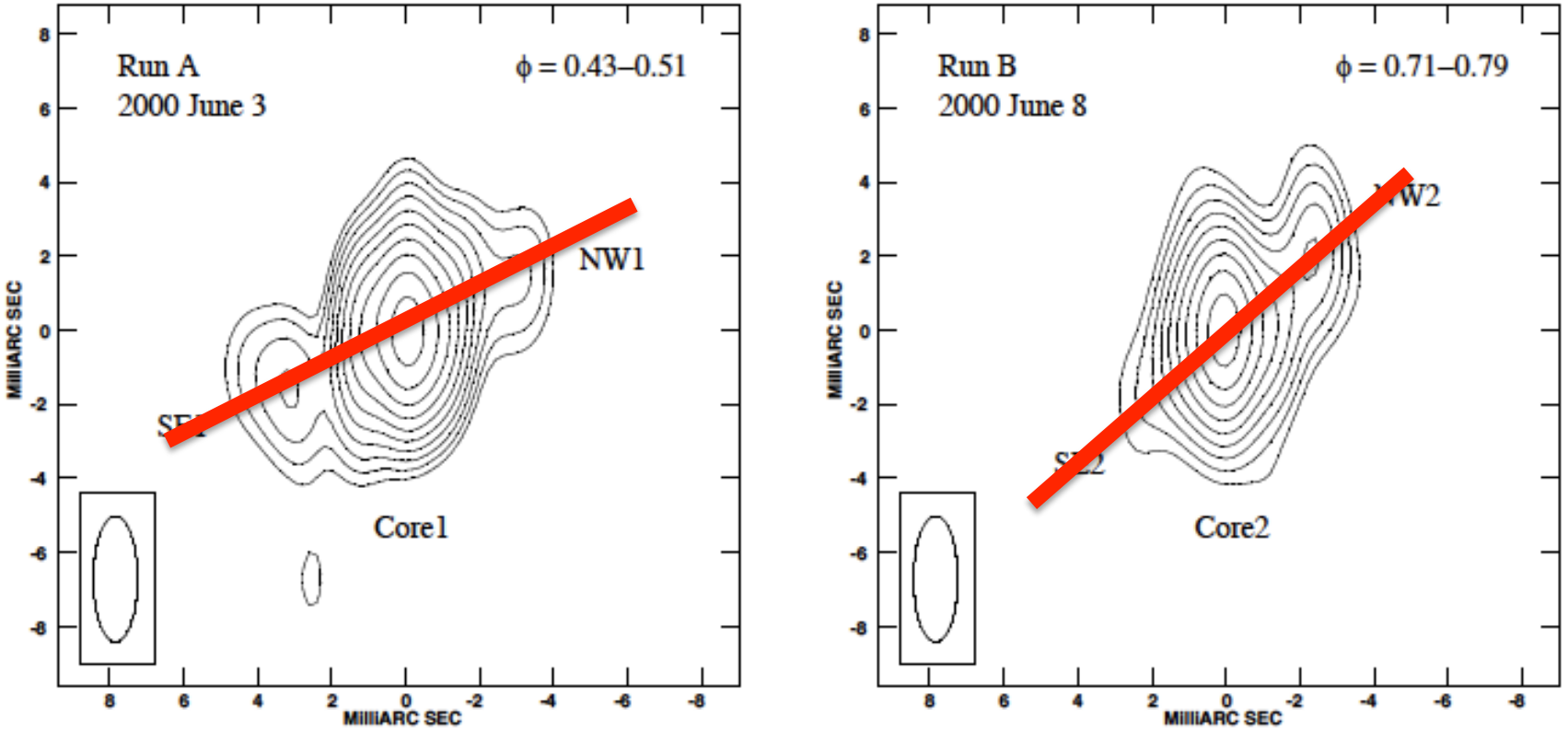

Fig. 1. VLBA+phased VLA self-calibrated images of LS 5039 at 5 GHz obtained on 2000 June 3 (left) and 8 (right). North is up and east is to the left. Axes units are mas, and the (0,0) position corresponds to the source peak in each image. The convolving beam, plotted in the lower left corner, has a size of 3.4×1.2 mas in PA of 0°. The first contour corresponds to 5 times the rms noise of the image (0.08 and 0.11 mJy beam^{-1} for run A and B, respectively), while consecutive ones scale with $2^{1/2}$. The dates and orbital phases are quoted in the images. There is extended radio emission that appears nearly symmetric for run A and clearly asymmetric for run B, with a small change of ~10° in its position angle. We have labeled the components fitted to the data, the parameters of which are listed in Table 1.

M. Ribo et al. 2000

LS 5039のGeV-TeV比較

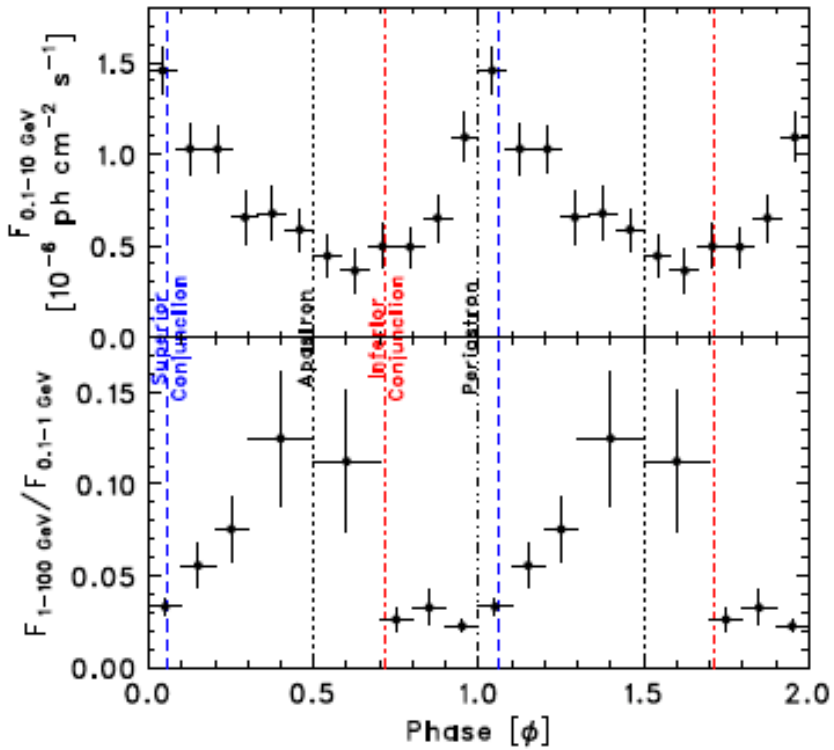

FIG. 5.— Top: flux vs. orbital phase for 0.1-10 GeV. Bottom: variatic with orbital phase in the hardness ratio of 1-100 to 0.1-1 GeV.

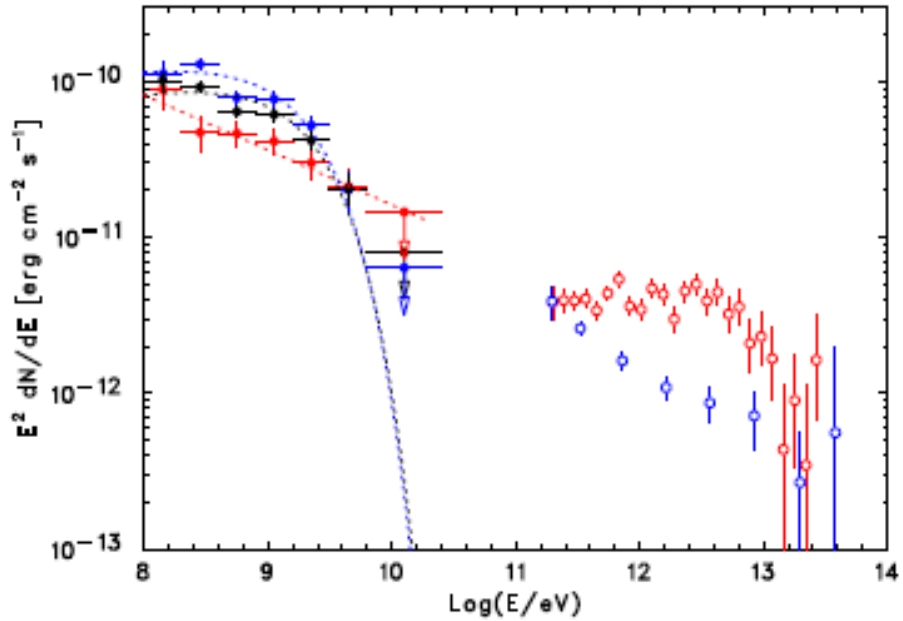

FIG. 3.— Fitted spectrum of LS 5039. Fermi data points are from likelihood fits in each energy bin. The black points (dotted line) represent the phase-averaged *Fermi*/LAT spectrum. The red data points (dotted line) represent the spectrum (overall fit) at inferior conjunction (Phase 0.45–0.9); blue data points (dotted line) represent the spectrum (overall fit) at superior conjunction (Phases, <0.45 and >0.9). Data points above 100 GeV are taken from H.E.S.S. observations (Aharonian et al. 2006); the data from H.E.S.S. are not contemporaneous with *Fermi*, though they do cover multiple orbital periods.

FERMI LAT OBSERVATIONS
ABDO et al. (2010)

LS 5039:周期放射 多波長

SUZAKU: 1-10 keV
KISHISHITA et al. 2009

Fermi: 0.1-10 GeV
ABDO et al. 2010

H.E.S.S.: > 1 TeV
Aharonian et al. 2006

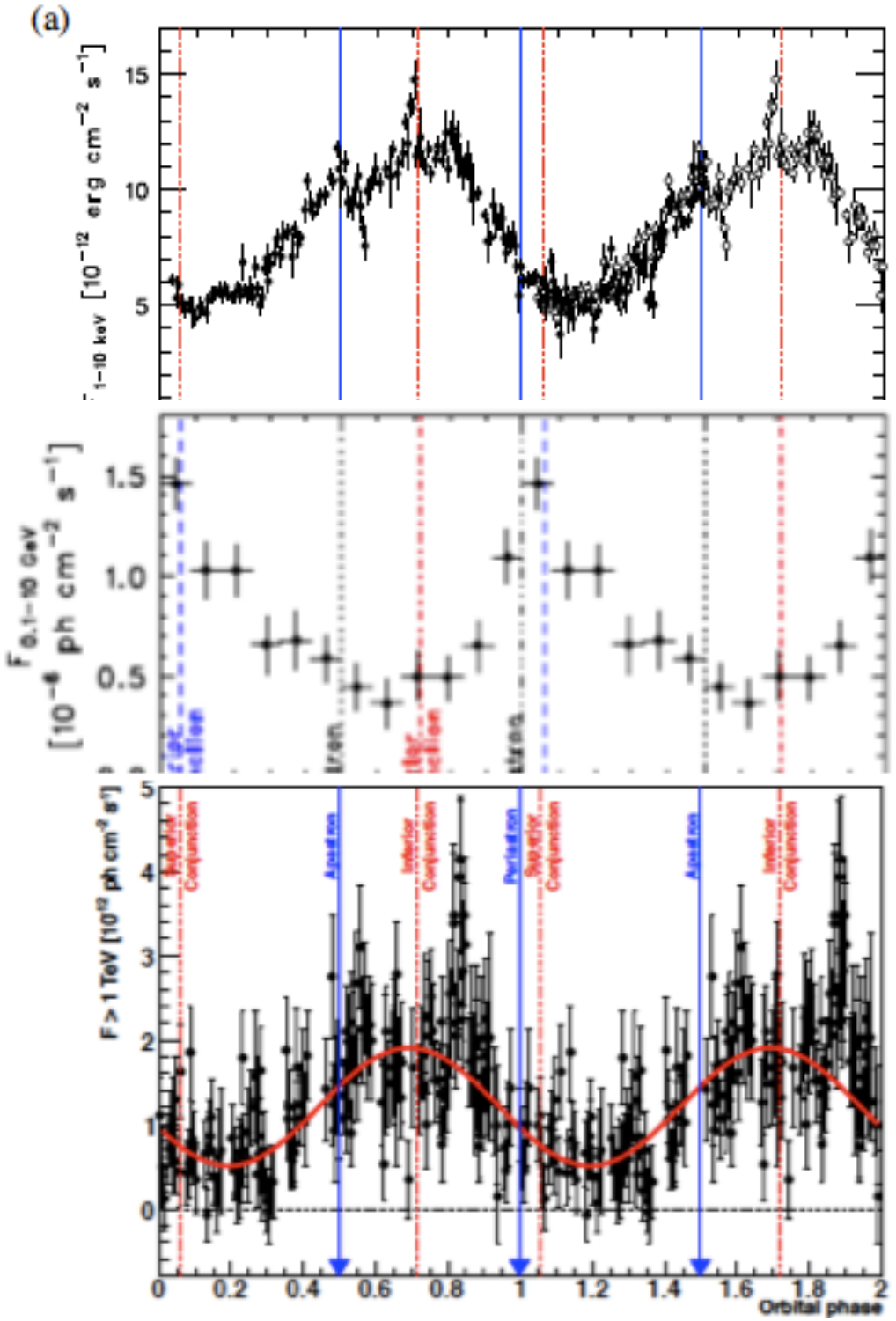

PSR B1259/SS2883:TeV

- スペクトル

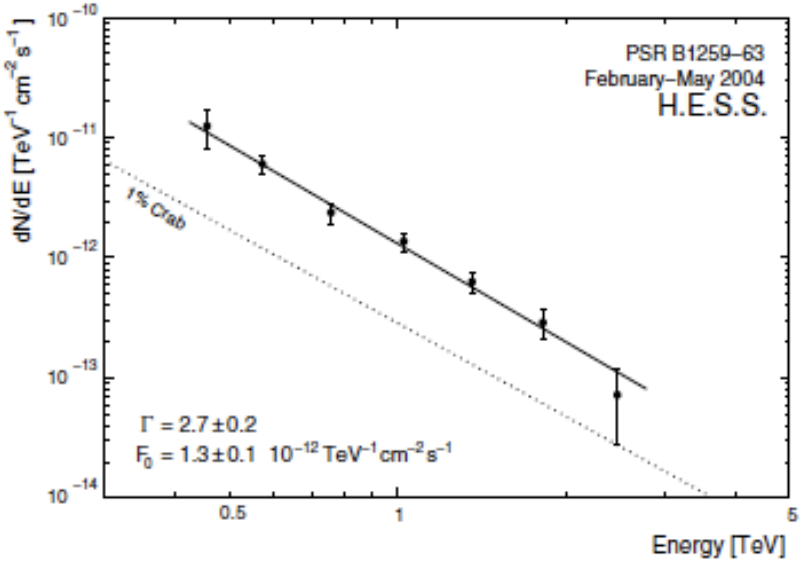

Period 2004	Γ	F_0 [TeV^{-1} cm^{-2} s^{-1}]	χ^2/ ndf	P_{χ^2}	E_{th} [GeV]
February	2.8 ± 0.3	$2.1 \pm 0.3 \times 10^{-12}$	1.8/4	0.77	370
March	3.0 ± 0.6	$1.0 \pm 0.2 \times 10^{-12}$	1.8/4	0.76	420
April	2.8 ± 0.4	$2.0 \pm 0.3 \times 10^{-12}$	0.4/3	0.93	350
Overall*	2.7 ± 0.2	$1.3 \pm 0.1 \times 10^{-12}$	2.3/5	0.81	380

* Includes all data from February to May 2004.

H.E.S.S.: Aharonian et al. 2005

- Light cureve

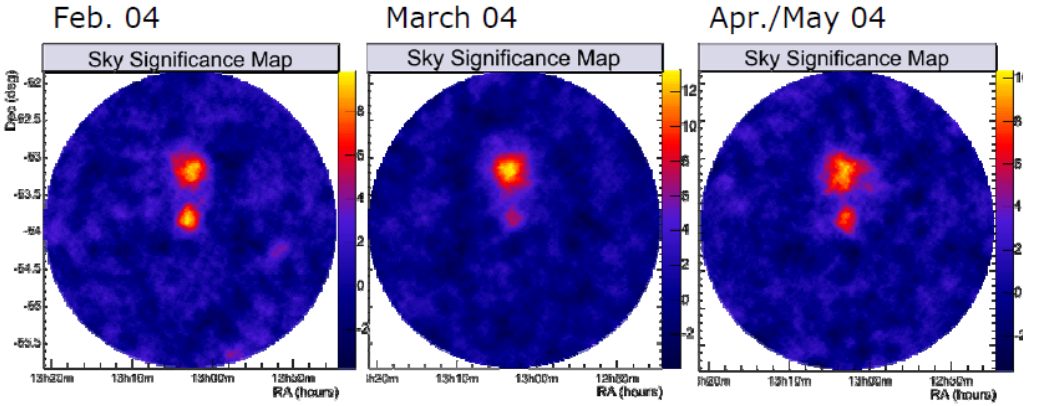

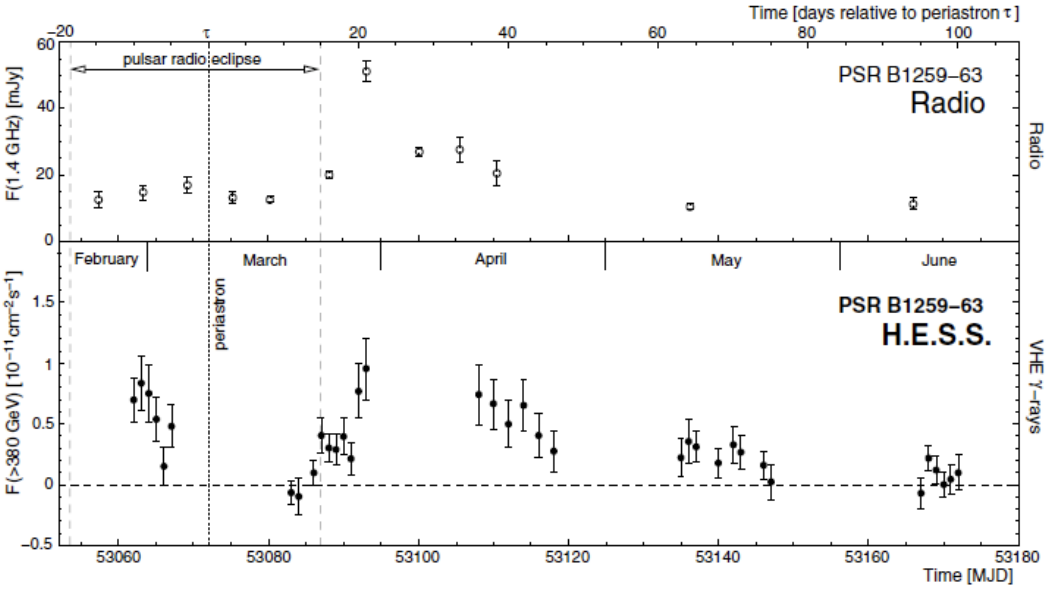

PSR B1259/SS2883：多波長観測

- 非熱的放射
- ふた山の放射ピーク
  - 近星点の前後
  - 非対称　電波ではひと山の時もある
- 放射ピークの時期
  - ピーク時期がpulsarがdisk面を通過する時に対応
  - 相互作用領域での衝撃波加速
  - TeV放射でdisk通過を決めることが出来る

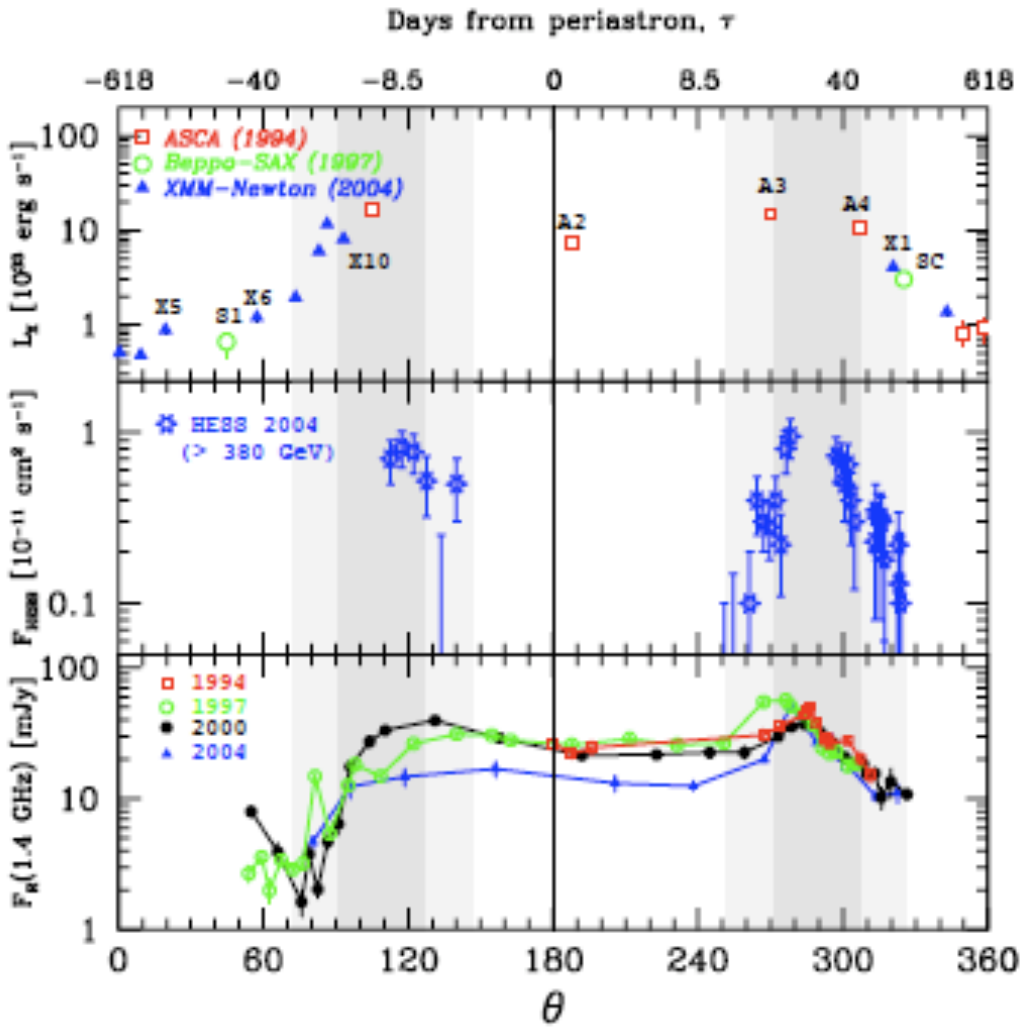

Fig. 1 Comparison between the X-ray (top), TeV (middle) and radio (bottom) lightcurves. *XMM-Newton* observations are marked with triangles, *Beppo*SAX ones with circles, and *ASCA* ones with squares. Data for four different periastron passages. are shown with different colors: red (1994), green (1997), black (2000) and blue (2004). Bottom X axis shows the orbital phase, θ, top X axis shows days from periastron, τ.

Neronov & Chernyakova 2006

3-D Numerical Simulations of the Binary System PSR B1259-63/SS 2883 and High Energy Emission from the DISK-Wind interaction Region

Tsuguya Naito collaboration with

A. Okazaki, S. Nagataki,

A. Kawachi, K. Hayasaki

@High Energy Phenomena in Massive Stars, University of Jaen 02/02/2009

PulsarとBe diskの相互作用を考える

- 潮汐力が働く
  - diskは生き残れるのか?
  - 相互作用は止まらないか？
- Pulsarに質量移入はおこるか？
  - 衝撃波モデルは不適

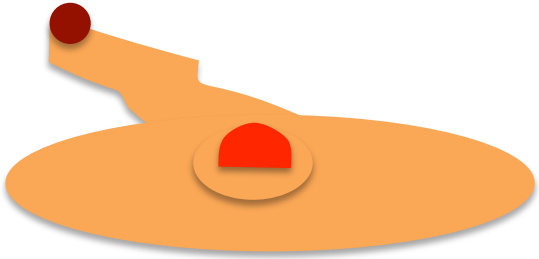

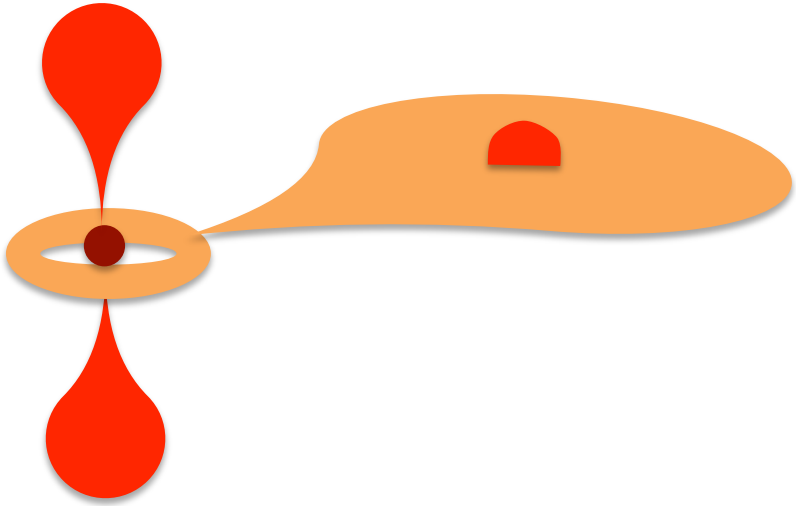

重力相互作用だけを考慮した3Dシミュレーション

PSRB1259/SS2883の NSとdiskの重力のみを 考慮したシミュレーション

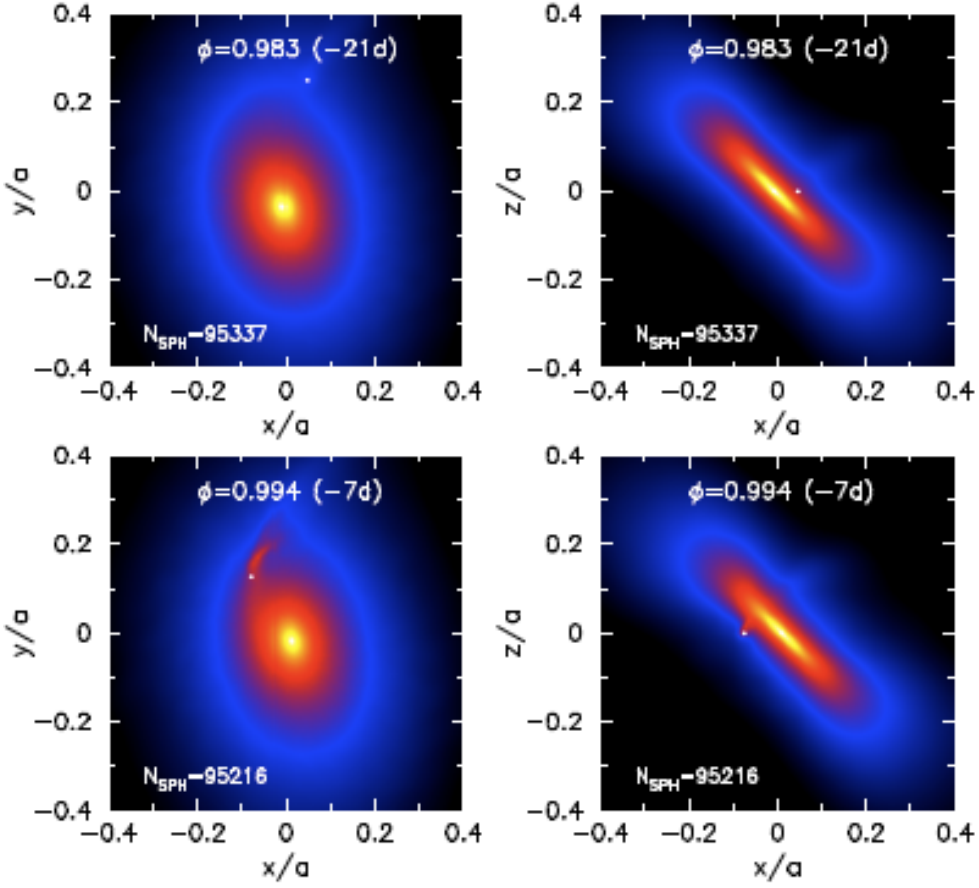

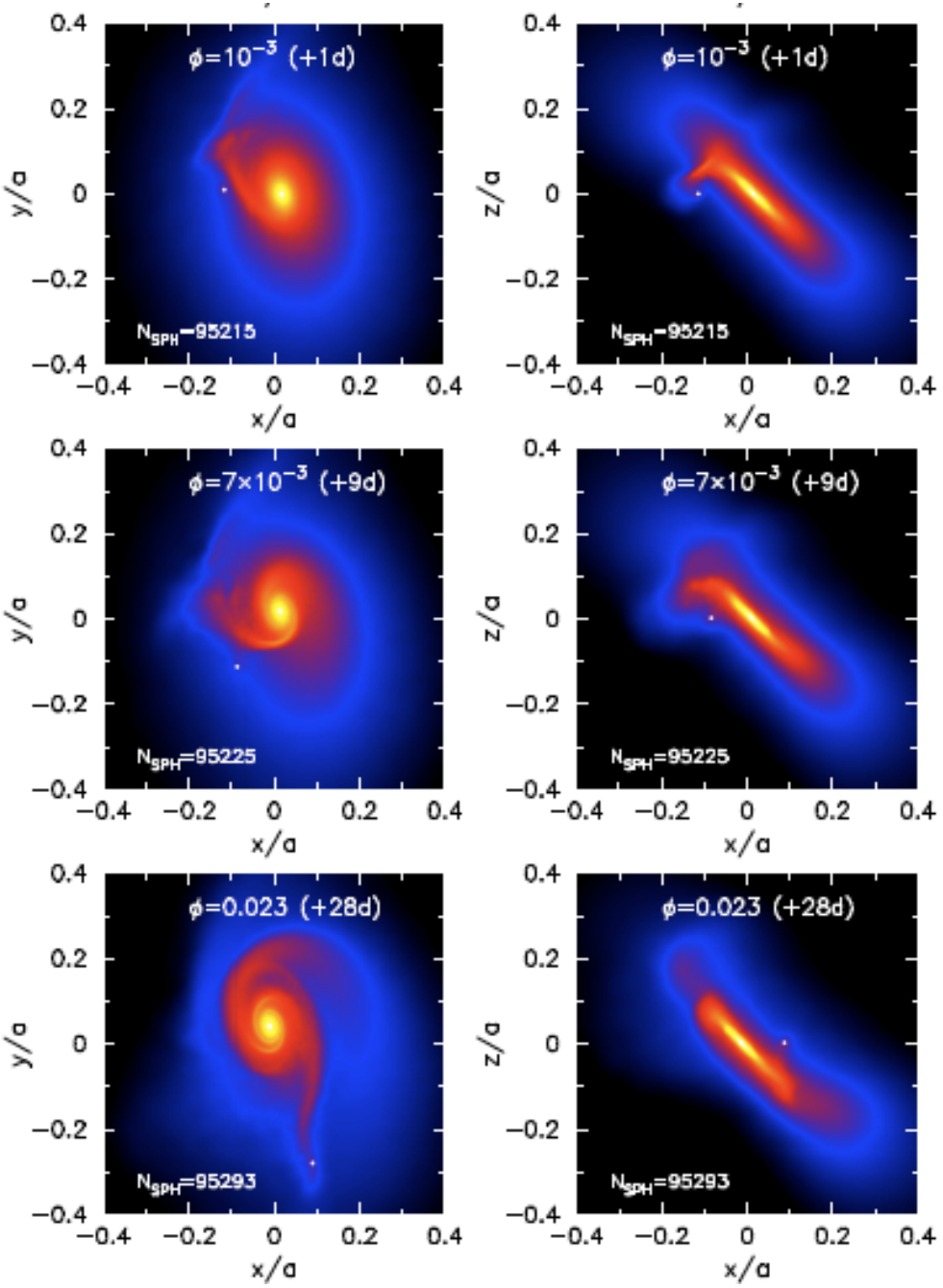

放射モデル

- 衝撃波による粒子加速
  - ベキ型スペクトル

$$\frac{dn_{\mathrm{e}}}{dE_{\mathrm{e}}} = n_0 E_{\mathrm{e}}^{-\alpha}$$

- Pulsar風中の電子が加速される
  - シンクロトロン放射
  - 逆コンプトン放射

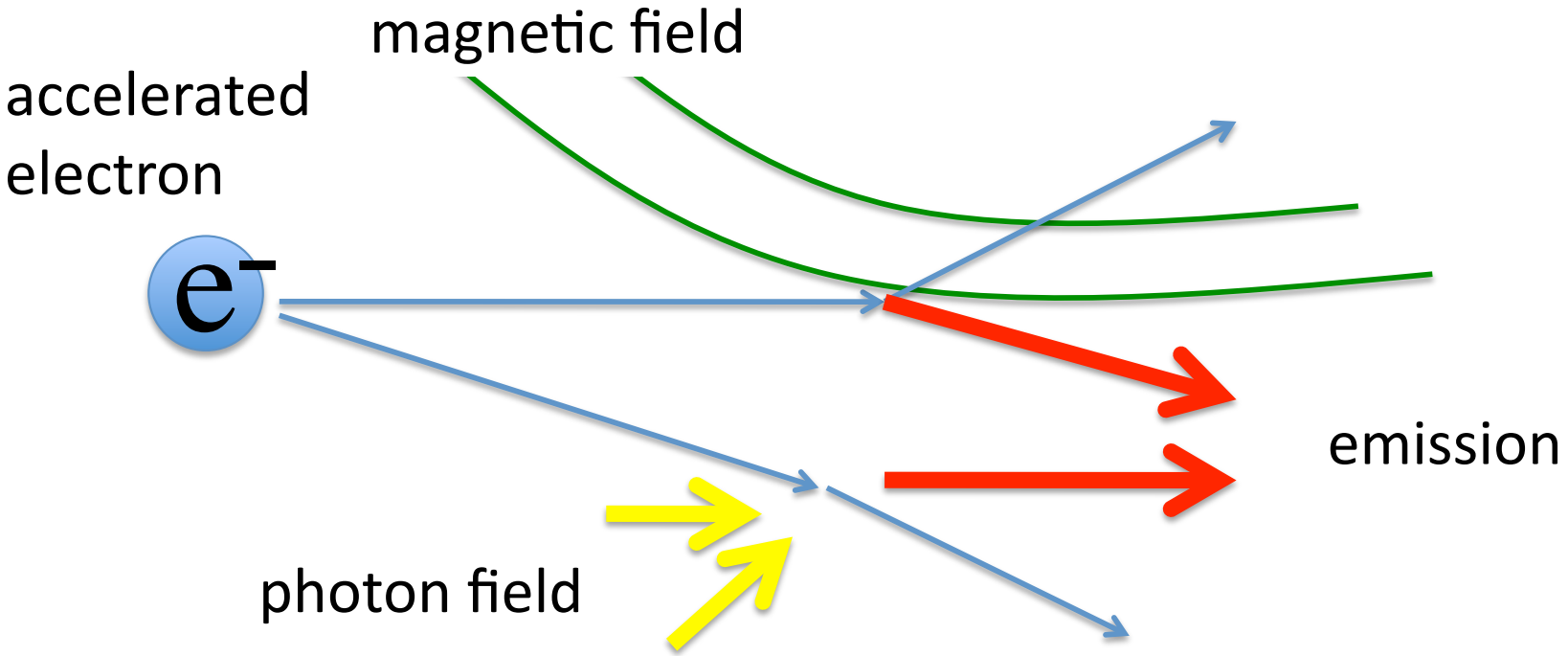

シンクロトロン放射

$$\frac{dF_\gamma}{dE_\gamma} = \frac{1}{4\pi D^2}\int dV \int dE_e \frac{dn_e}{dE_e}\frac{B^2}{8\pi}\upsilon_e \frac{d\sigma_{\mathrm{sync}}(E_e, E_\gamma)}{dE_\gamma}$$

- 磁場
  - パルサー磁場の標準的なモデル

$$B \propto r_{\mathrm{ns}}^{-1}$$

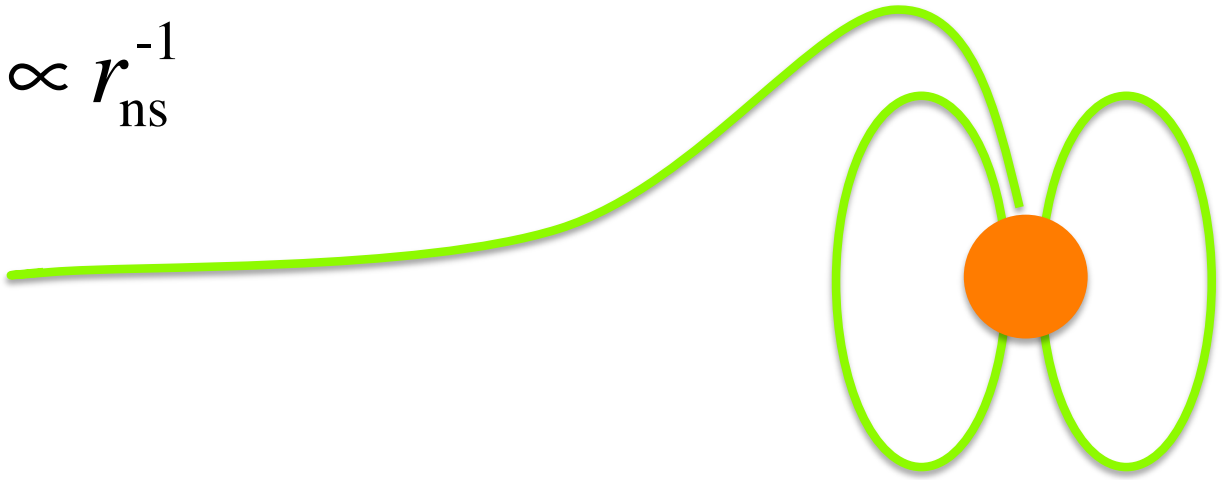

逆コンプトン放射

$$\frac{dF_\gamma}{dE_\gamma} = \frac{1}{4\pi D^2}\int dV \int dE_e \int d\nu \frac{dn_{\mathrm{e}}}{dE_{\mathrm{e}}} u(\nu)\upsilon_{\mathrm{e}} \frac{d\sigma_{\mathrm{IC}}(E_e, E_\gamma, \nu)}{dE_\gamma}$$

- 種光子　$u(\nu)$
  - Be星からの放射
  - 2.7 K CMB（宇宙背景放射）
  - 銀河内の背景放射

$$u(\nu) = \frac{8\pi\nu^2}{c^3}\frac{1}{\exp(h\nu/kT)-1}$$ CMB, 銀河背景

$$= \frac{1}{4}\frac{R_*^{\,2}}{r_{Be}^2}\frac{8\pi\nu^2}{c^3}\frac{1}{\exp(h\nu/kT)-1}$$ Be星

放射領域

- Be dsikの圧力とPulsar windの圧力がつり合う面
  - Pulsar windを仮定する
  - 接触不連続面
  - 衝撃波
- 最も圧力が大きい位置
  - 放射が最大の領域
  - 今回はこの周辺を考える
- 粒子加速

$$\frac{dn_{\mathrm{e}}}{dE_{\mathrm{e}}} = n_0 E_{\mathrm{e}}^{-\alpha} \propto P_{\mathrm{local}}$$

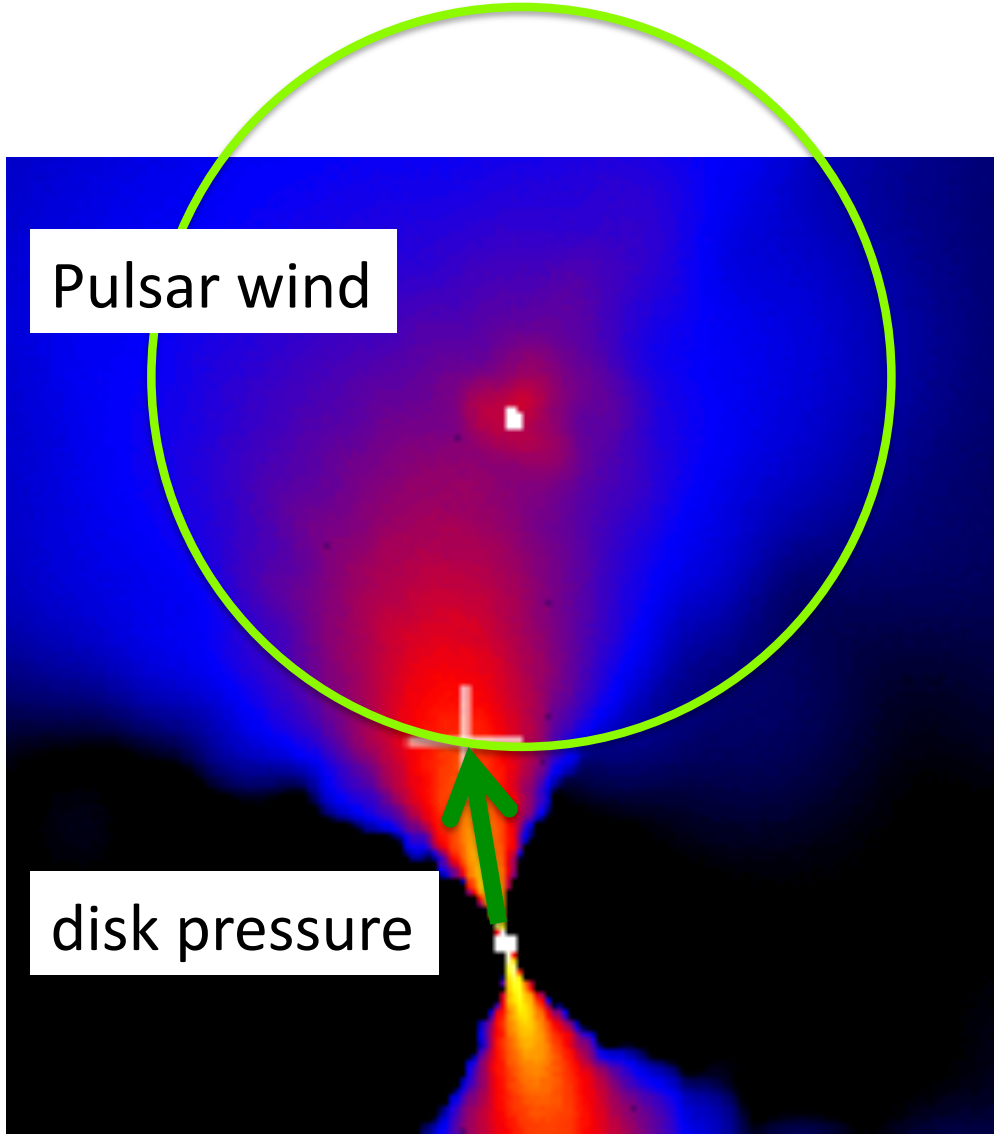

観測を説明する高エネルギー放射の energy spectrumモデル

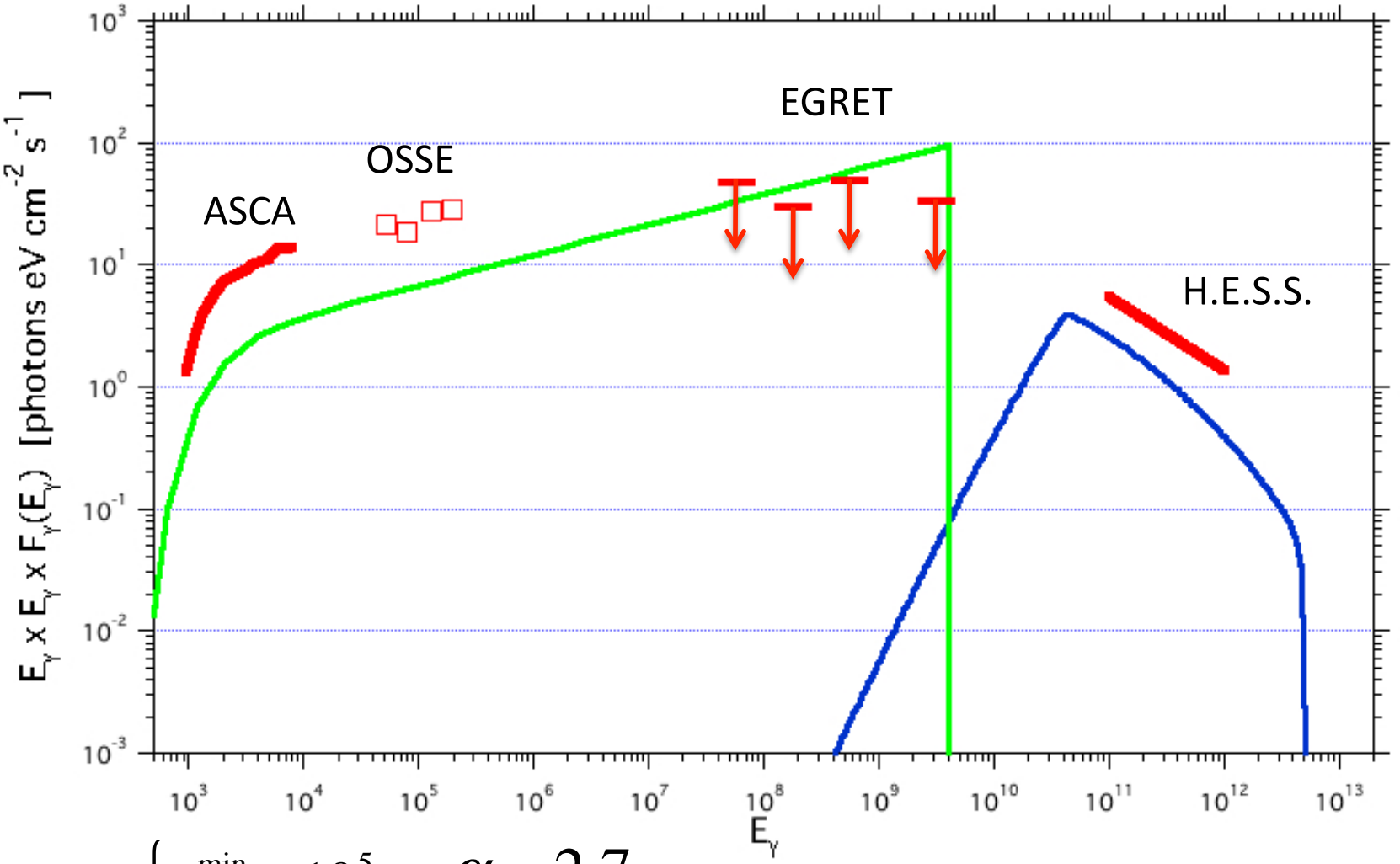

$$\begin{cases} \gamma_e^{\min} = 10^5 \\ \gamma_e^{\max} = 10^7 \end{cases} \qquad \alpha = 2.7$$

Light curve

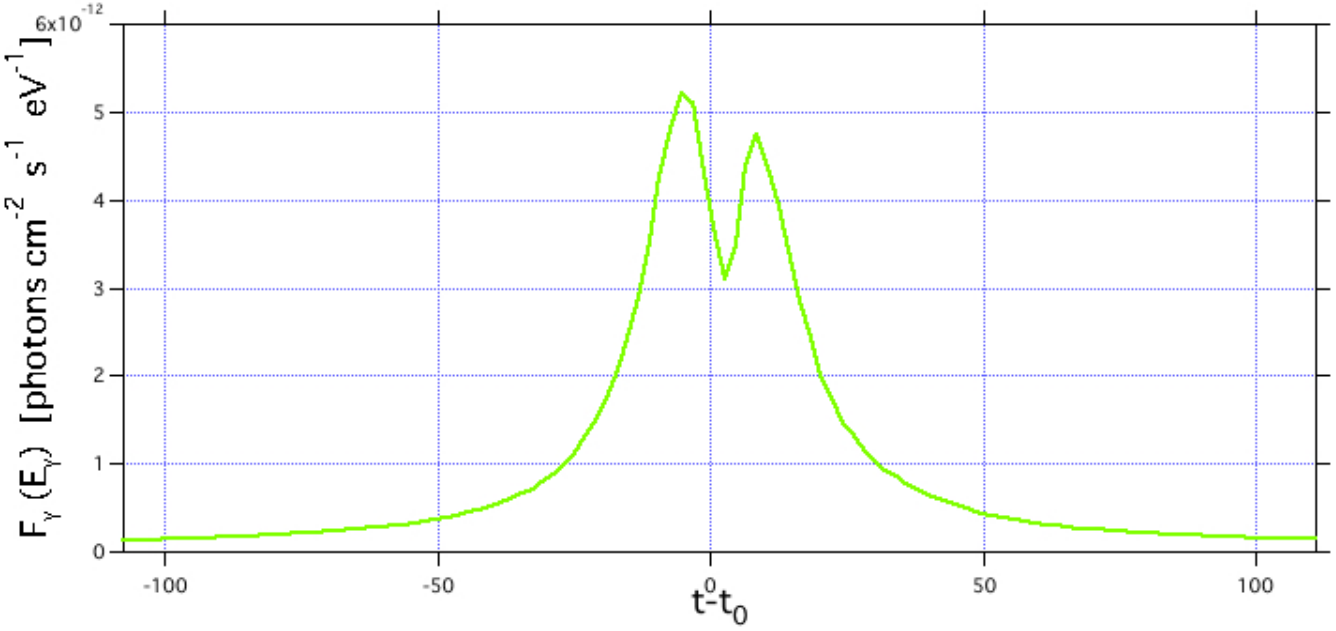

Synchrotron
X-ray –
GeV gamma-ray

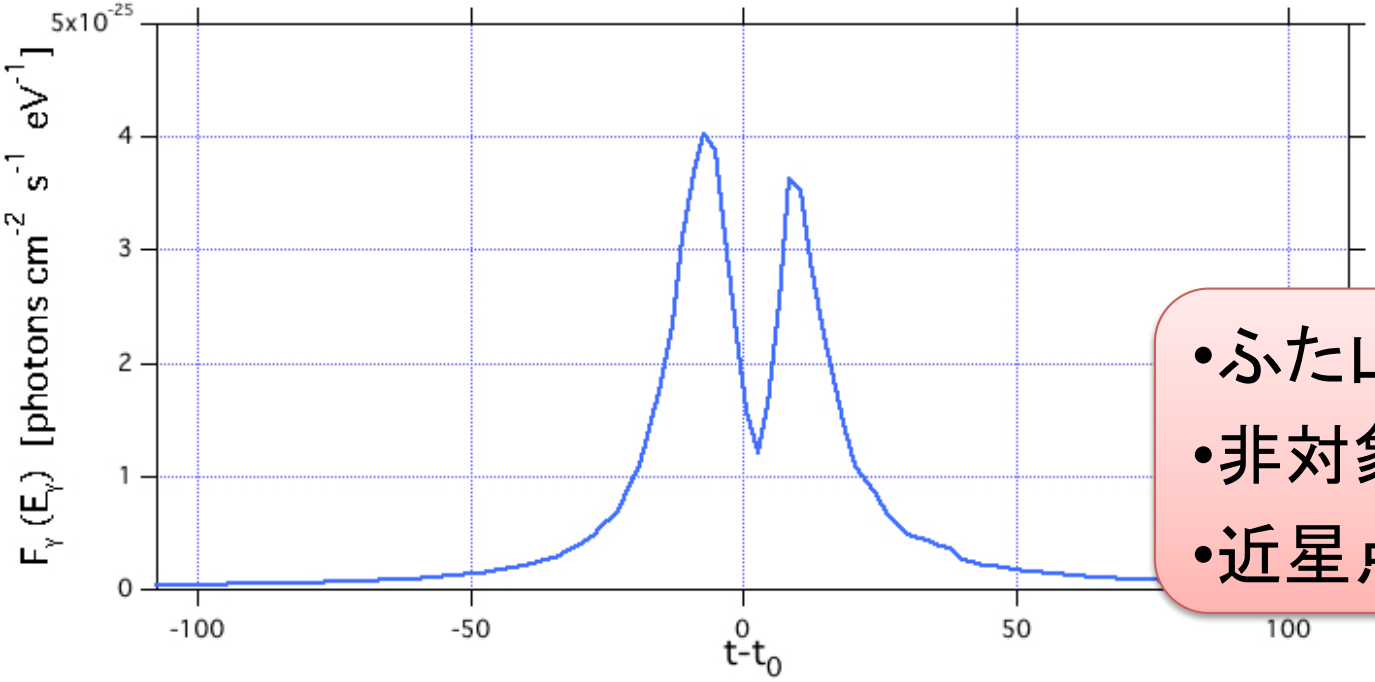

Inverse Compton
TeV gamma-ray

- ふた山のピークを再現
- 非対象性の再現
- 近星点でも放射がある

pulsarがdiskの中心面
付近を通過中

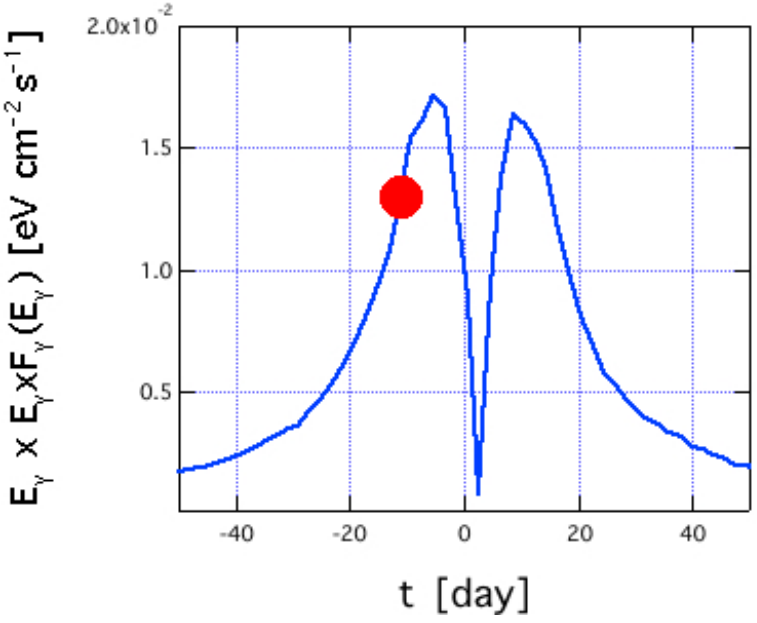

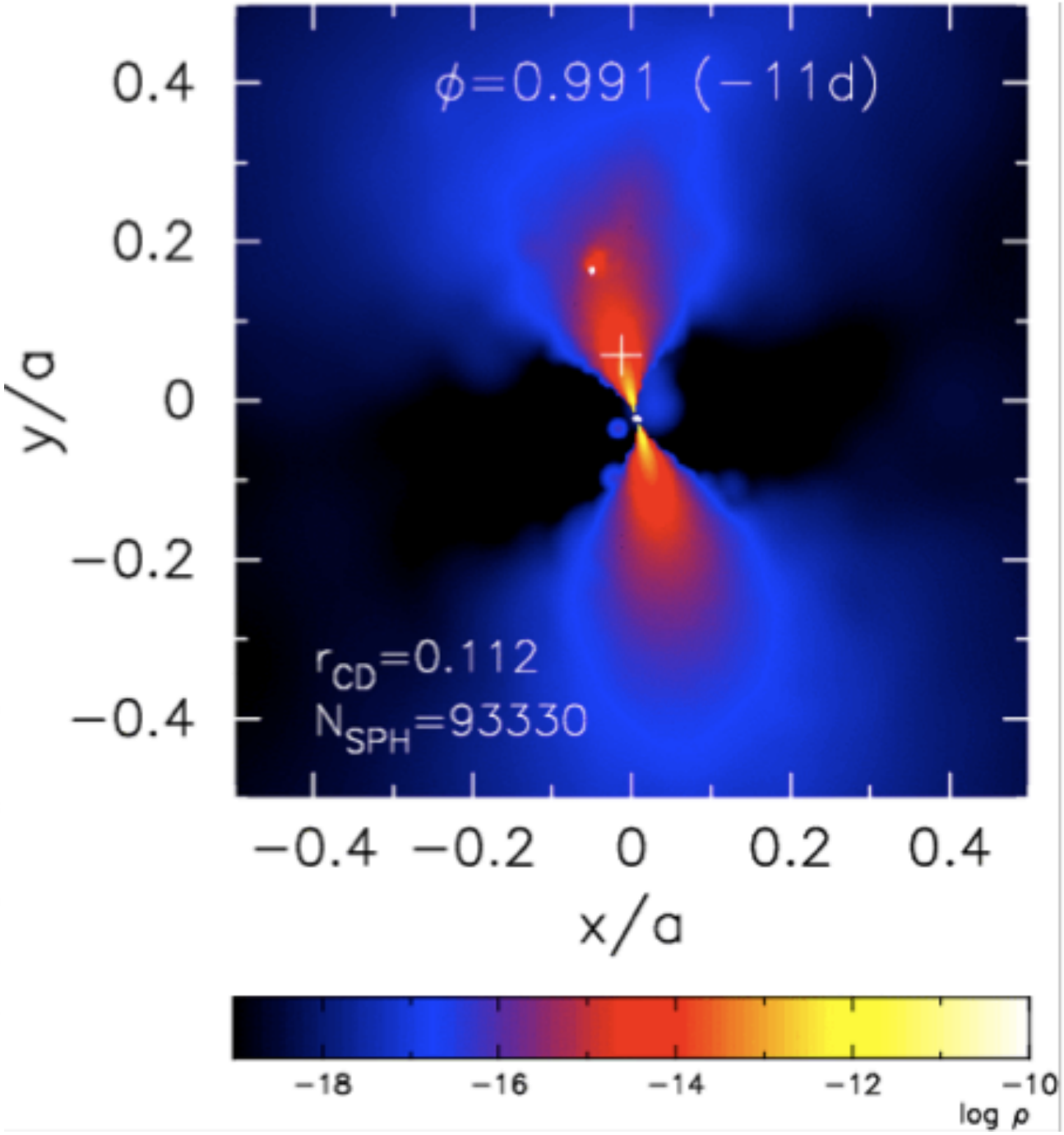

放射のピーク

pulsarのdisk通過が放射のピークではない

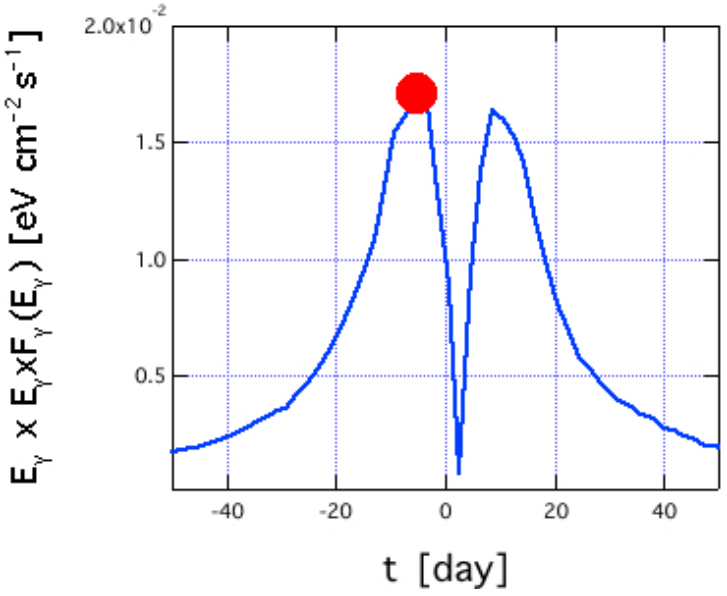

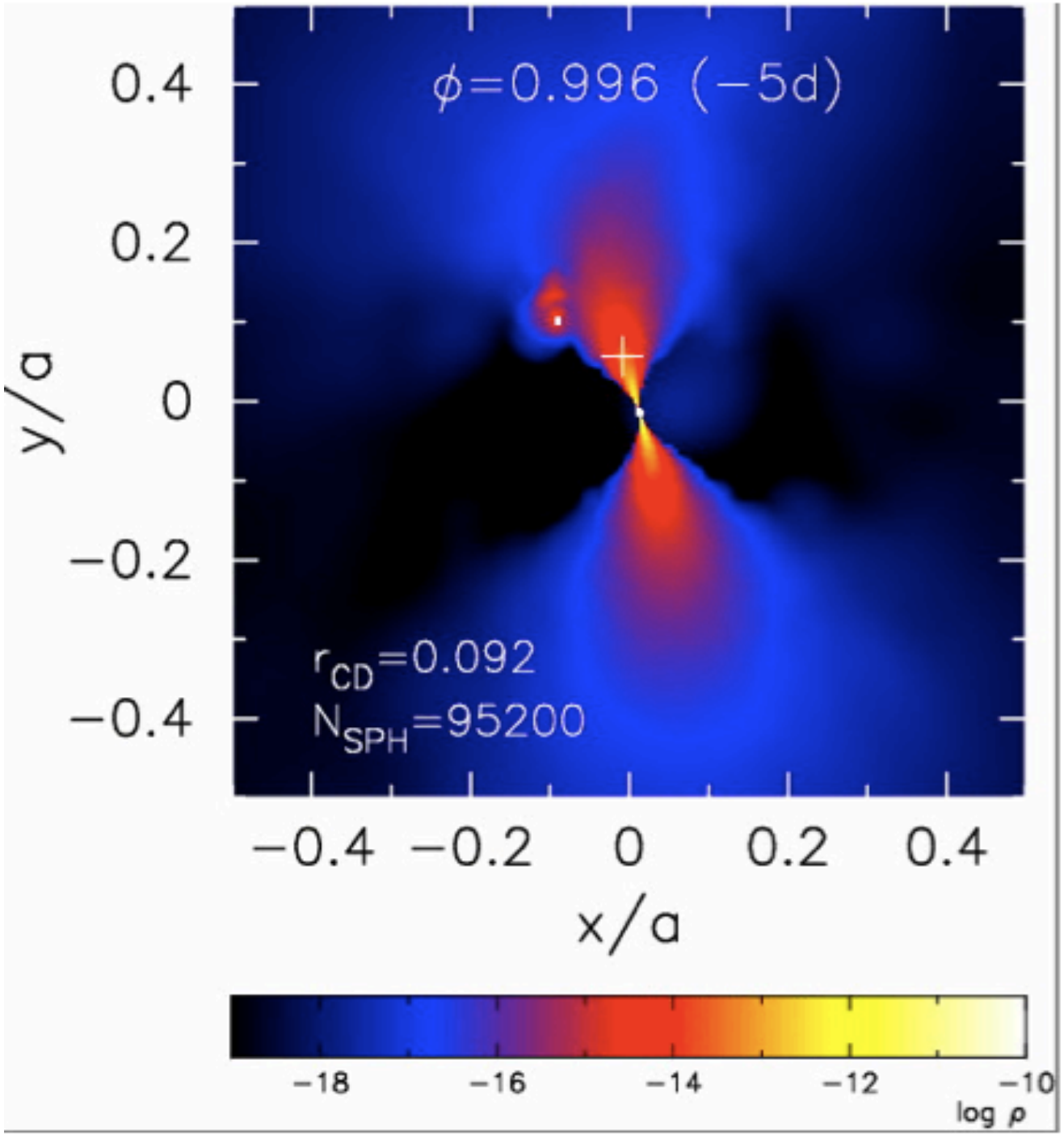

PSR B1259-63/SS2883: 近星点

- 2007年の観測
  - H.E.S.S.
  - CANGAROO
    - 隣のTeVソースの影響が大きい

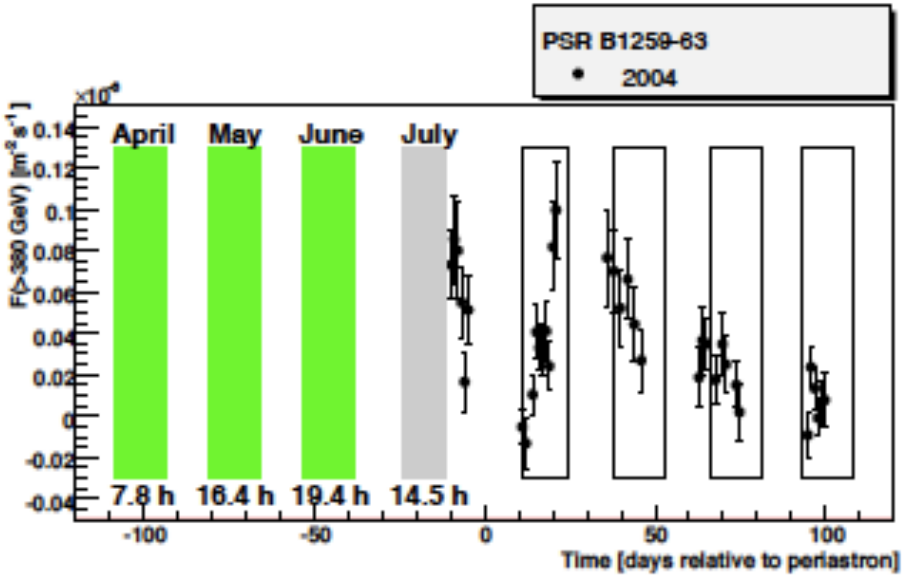

Figure 4: *The PSR B1259−63 observation windows in 2007 for zenith angles* $< 45°$ *with respect to the system's time relative to periastron. Green boxes indicate that data taking has already been accomplished during the corresponding month. The empty boxes are the 2007 observation windows mirrored with respect to periastron, overlayed with the 2004 data for comparison.*

H.E.S.S. KERSCHHAGGL et al. (2008)

新しいTeV binaryソース

- HESS J0632+057

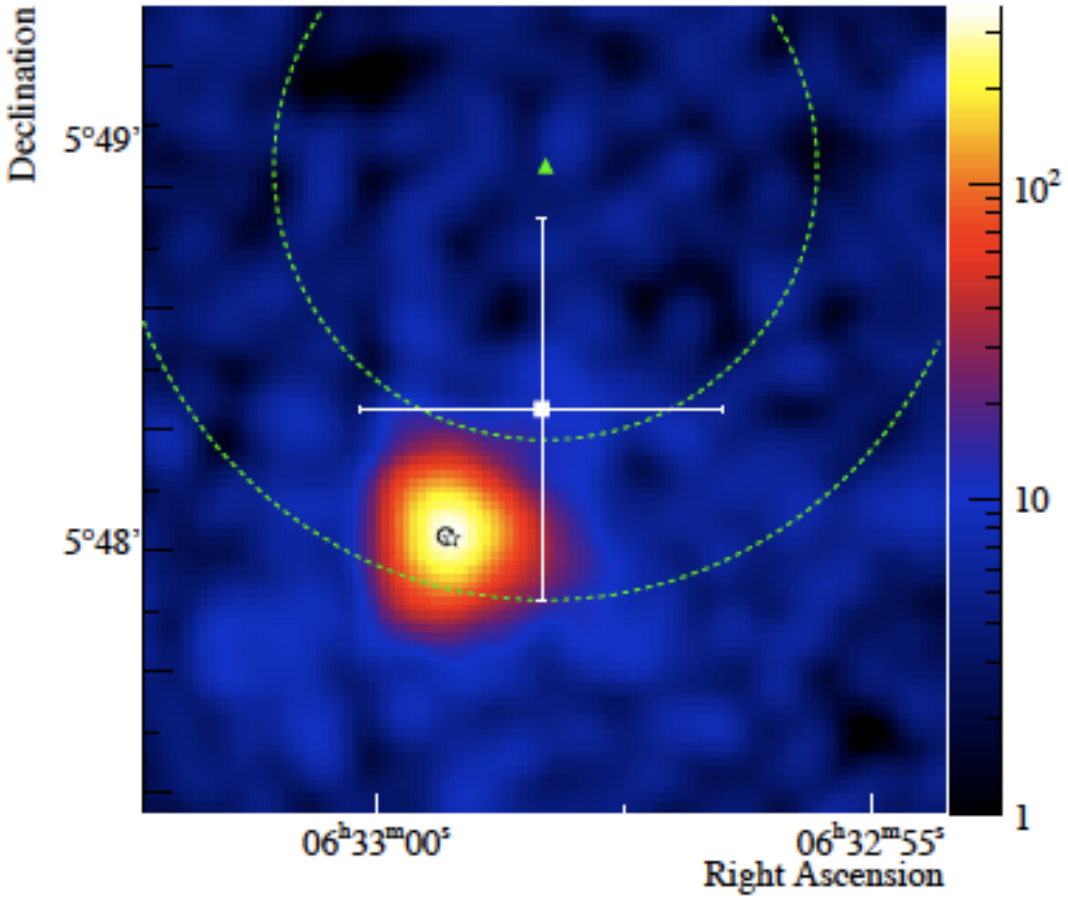

Acciari et al. (2010)

← XMM-Newton combined MOS-1/MOS-2

□ HESS J0632+057

○ XMMUJ063259.3+054801

☆ MWC148 (Be star: spectral type B0pe)

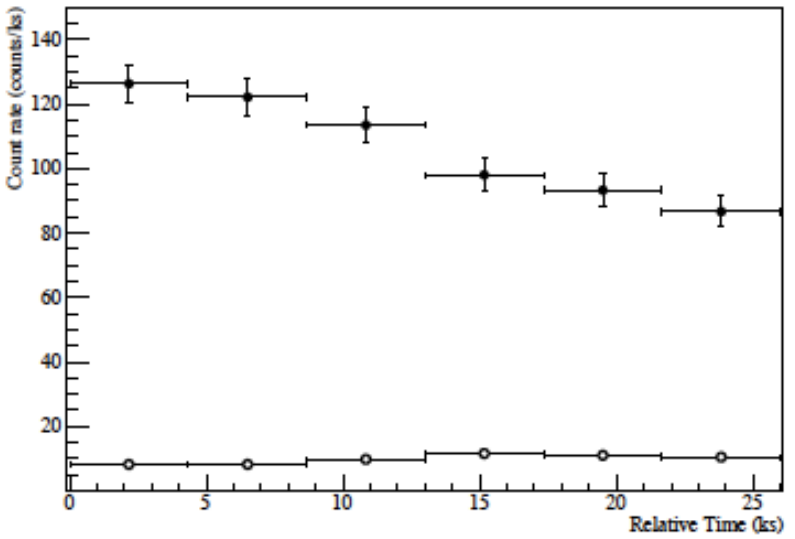

FIG. 3.— X-ray light-curve for XMMU J063259.3+054801 for the combined EPIC cameras. Background-subtracted signal (closed circles) and estimated background (open circles) are shown.

XMMUJ063259.3+054801
のフラックスが時間変化している →

The radio counterpart of the likely TeV binary HESS J0632+057

J.L. Skilton[1⋆], M. Pandey-Pommier[2], J.A. Hinton[1], C.C. Cheung[3], F.A. Aharonian[4], J. Brucker[5], G. Dubus[6], A. Fiasson[7,8], S. Funk[9], Y. Gallant[7], A. Marcowith[7], O. Reimer[9,10]

Name	D (kpc)	$L_{\rm r}$	$L_{\rm X}$	$L_{\rm GeV}$*	$L_{\rm TeV}$	$\alpha_{\rm r}$	$\alpha_{\rm X}$	α_γ
LS 5039	2.5	1.3	5–50	70	4–11	0.46[⊕]	0.45 – 0.6[⊘]	0.9 – 1.5[⋈]
LS I +61 303	2.0	1–17	3–9	60	8	-0.6 – 0.45[†]	0.53[‡]	1.6 ± 0.2[♯]
PSR B1259-63	1.5	0.02–0.3	0.3–6	...!	2.3	-2.2 – 0.3[ΙΙ]	0.78[•]	1.7 ± 0.2[+]
Cygnus X-1	2.2	0.3	10^4	...!	12	0.1[◦]	0.8[⋆]	2.2 ± 0.6
HESS J0632+057	1.5	0.003	0.13[△]	<9	0.9[⊗]	0.6	0.26[△]	1.5 ± 0.3[⊗]

Table 1. Properties of the TeV emitting binaries, adapted from Paredes (2008). Note that the spectral indices are defined by $F_\nu \propto \nu^{-\alpha}$ or equivalently $dN/dE \propto E^{-(1+\alpha)}$. All luminosities are in units of 10^{33}erg s^{-1} except the radio luminosities which are in units of 10^{31}erg s^{-1}. Luminosities are given for the following ranges: $L_{\rm r}$: 0.1 –100 GHz, $L_{\rm X}$: 1 – 10 keV, $L_{\rm GeV}$: 1 – 10 GeV, $L_{\rm TeV}$: 0.2 – 10 TeV. [⊕]Marti et al. (1998), [⊘]Takahashi et al. (2009), [⋈]Aharonian et al. (2006), [†]Gregory (2002), [‡]Albert et al. (2006), [♯]Albert et al. (2009), [ΙΙ]Johnston et al. (2005), [•]Esposito et al. (2007), [+]Aharonian et al. (2005b), [◦]Pandey et al. (2007), [⋆]Miller et al. (2005), [△]Hinton et al. (2009), [⊗]Aharonian et al. (2007). *GeV luminosity measurements are from the Fermi Bright Source List (Abdo et al. 2009), with upper limits estimated from non-detection at a 10σ level after three months of observations. Note that the association of GeV emission with LS 5039 is based only on positional coincidence. [!]No GeV detection reported yet.

電波源であることがPoint？

新たなTeV binary発見の可能性

- 5つの天体の共通点
  →HMXBs
  - 電波で観測されている
    - 軌道周期
  - jet天体
    jet-wind, jet-clump

$$L_\gamma \propto v_w{}^2 \dot{M}_{MS} \propto \frac{M_c}{R}$$

  - disk相互作用

$$L_\gamma \propto \dot{E}_{NS}$$

- X線連星
  - HMXBs　114天体
    - 9天体が電波源
  - LMXBs　186天体
    - 55天体が電波源
- Be starとNSの連星系
  - HMXBs
- 大質量星の連星
  - ～100$M_\odot$

X線連星

- HMXBs　114天体
  - ２種類に分けられる
    - Be star　→　Roche lobeを満たしていない
    - OB SG stars　→　Roche lobeを満たし質量移入が進行
  - 9天体が電波源
    6 persistent and 3 transient sources
- LMXBs　186天体
  - 多くがRoche lobeを満たし質量移入が進行
  - 55天体が電波源
    18 persistent and 37 transient sources

HMXBs

- Gamma-ray Binary > 24 sources

name	distance (kpc)	
4U 0352+30	1.3	
H1145-619	1.5	2E 1145.5-6155
GX 301-2	1.8 ± 0.4	
Vela X-1	2	
H1907+097	2.4-5.9	
A1118-616	4	

- SAX J0635+0533
  - pulsar 33.8 ms: X-ray, radio
  - GeV : 2EG J063510521 (Thompson et al. 1995)
  - Massive Star → Be star (Kaaret etal. 1999)

大質量星連星

- eta Carina
  - 少なくとも2個以上星からなる連星系

$$\dot{M} \approx 10^{-4}\ [M_{\odot}\ \mathrm{yr}^{-1}]$$

$$v_{\infty} \approx 2000\ [\mathrm{km\ s}^{-1}]$$

$$L_{\mathrm{wind}} \approx 2.5 \times 10^{38}\ [\mathrm{erg\ s}^{-1}]$$

RXTE: CORCORAN (2001)

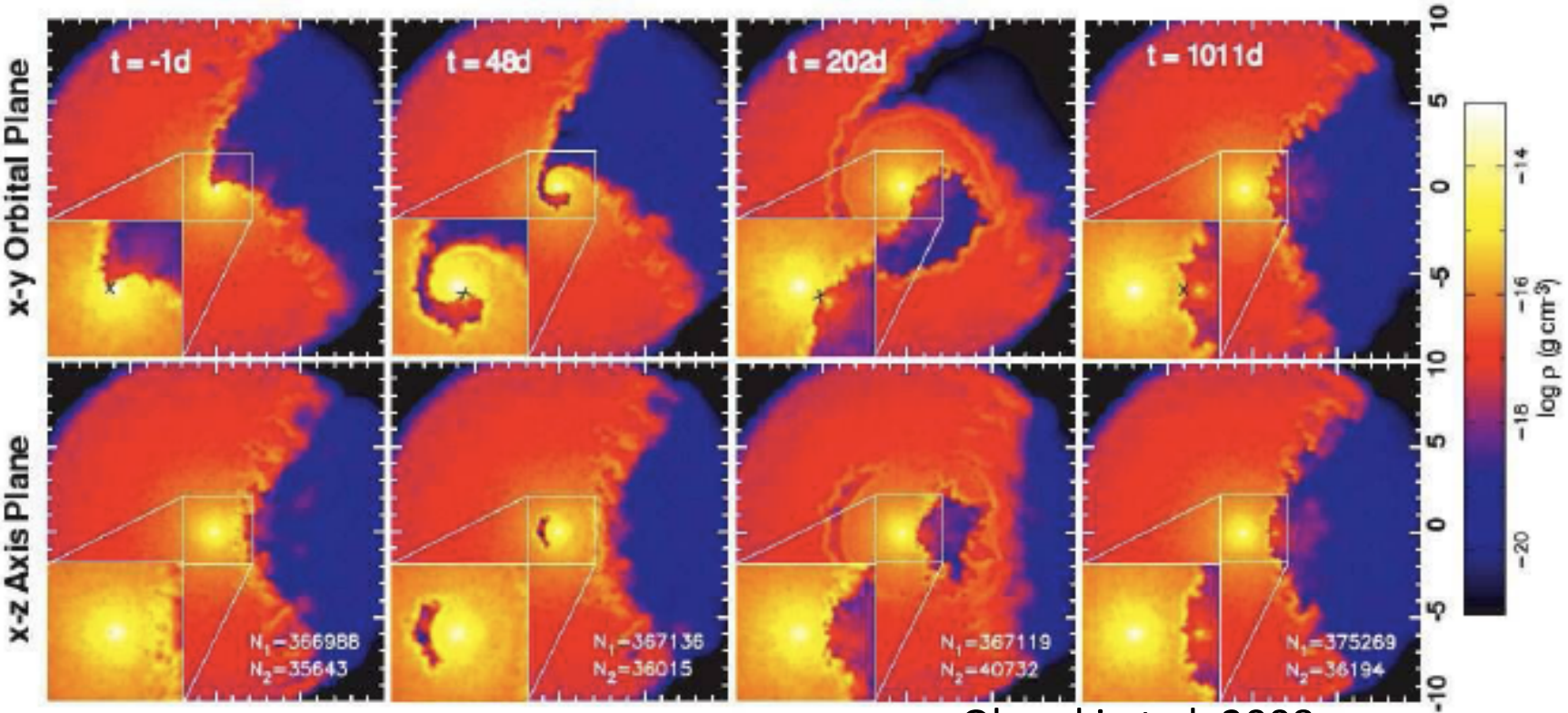

Okazaki et al. 2008

まとめ

- ４つの連星系
  - LS I +61 303のjet、flare
  - LS 5039のGeV-TeVの逆相関
  - PSR B1259−63/SS2883のdisk-PW model
  - Cygnus X-1
- 新しいTeVソース
  - HESS J0632+057
- 未知のTeVソースの可能性
  - HMXBs
    - SAX J0635+0533 (Be-star)
  - Massive star Binary
    - eta Carina